AD-A093 553 FEDERAL AVIATION ADMINISTRATION TECHNICAL CENTER ATL--ETC F/G 17/7
MICROWAVE LANDING SYSTEM (MLS) CLEARANCE FORMAT ASSESSMENT TEST--ETC(U)
DEC 80 R MCFADDEN
UNCLASSIFIED FAA-CT-80-46 NL

1 OF 1

END
DATE
FILMED
DTIC

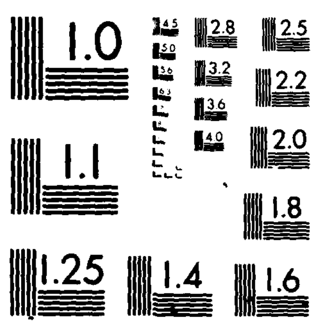

MICROCOPY RESOLUTION TEST CHART
NATIONAL BUREAU OF STANDARDS-1963-A

Report No. FAA-CT-80-46

(12)

MICROWAVE LANDING SYSTEM (MLS) CLEARANCE FORMAT ASSESSMENT TESTS

Robert McFadden

DATA REPORT

DECEMBER 1980

Document is available to the U.S. public through the National Technical Information Service, Springfield, Virginia 22161

Prepared for

U. S. DEPARTMENT OF TRANSPORTATION
FEDERAL AVIATION ADMINISTRATION
TECHNICAL CENTER
Atlantic City Airport, New Jersey 08405

NOTICE

Technical Report Documentation Page

1. Report No.	2. Government Accession No.	3. Recipient's Catalog No.
FAA-CT-80-46	AD-A093 553	

4. Title and Subtitle
MICROWAVE LANDING SYSTEM (MLS) CLEARANCE FORMAT ASSESSMENT TESTS.

5. Report Date
December 1980

6. Performing Organization Code

7. Author(s)
Robert McFadden

8. Performing Organization Report No.
FAA-CT-80-46

9. Performing Organization Name and Address
Federal Aviation Administration
Technical Center
Atlantic City Airport, New Jersey 08405

10. Work Unit No. (TRAIS)

11. Contract or Grant No.
075-725-470

12. Sponsoring Agency Name and Address
U.S. Department of Transportation
Federal Aviation Administration
Technical Center
Atlantic City Airport, New Jersey 08405

13. Type of Report and Period Covered
Data Report
January — February 1980

14. Sponsoring Agency Code

15. Supplementary Notes

16. Abstract

This data report documents the Microwave Landing System (MLS) clearance format assessment tests performed at the Federal Aviation Administration Technical Center from January through February 1980. The test data were provided for inclusion in the United States presentation for the International Civil Aviation Organization (ICAO) All-Weather Operation Panel-8 meeting in Montreal in March 1980.

17. Key Words
Microwave Landing System
MLS Clearance Format Assessment Tests
Scanning Beam
Out of Coverage Indication
Azimuth Subsystem

18. Distribution Statement
Document is available to the U.S. public through the National Technical Information Service, Springfield, Virginia 22161

19. Security Classif. (of this report)	20. Security Classif. (of this page)	21. No. of Pages	22. Price
Unclassified	Unclassified	54	

Form DOT F 1700.7 (8-72) Reproduction of completed page authorized

METRIC CONVERSION FACTORS

Approximate Conversions to Metric Measures

Symbol	When You Know	Multiply by	To Find	Symbol
		LENGTH		
in	inches	*2.5	centimeters	cm
ft	feet	30	centimeters	cm
yd	yards	0.9	meters	m
mi	miles	1.6	kilometers	km
		AREA		
in^2	square inches	6.5	square centimeters	cm^2
ft^2	square feet	0.09	square meters	m^2
yd^2	square yards	0.8	square meters	m^2
mi^2	square miles	2.6	square kilometers	km^2
	acres	0.4	hectares	ha
		MASS (weight)		
oz	ounces	28	grams	g
lb	pounds	0.45	kilograms	kg
	short tons (2000 lb)	0.9	tonnes	t
		VOLUME		
tsp	teaspoons	5	milliliters	ml
Tbsp	tablespoons	15	milliliters	ml
fl oz	fluid ounces	30	milliliters	ml
c	cups	0.24	liters	l
pt	pints	0.47	liters	l
qt	quarts	0.95	liters	l
gal	gallons	3.8	liters	l
ft^3	cubic feet	0.03	cubic meters	m^3
yd^3	cubic yards	0.76	cubic meters	m^3
		TEMPERATURE (exact)		
°F	Fahrenheit temperature	5/9 (after subtracting 32)	Celsius temperature	°C

*1 in = 2.54 (exactly). For other exact conversions and more detailed tables, see NBS Misc. Publ. 286, Units of Weights and Measures, Price $2.25, SD Catalog No. C13.10:286.

Approximate Conversions from Metric Measures

Symbol	When You Know	Multiply by	To Find	Symbol
		LENGTH		
mm	millimeters	0.04	inches	in
cm	centimeters	0.4	inches	in
m	meters	3.3	feet	ft
m	meters	1.1	yards	yd
km	kilometers	0.6	miles	mi
		AREA		
cm^2	square centimeters	0.16	square inches	in^2
m^2	square meters	1.2	square yards	yd^2
km^2	square kilometers	0.4	square miles	mi^2
ha	hectares (10,000 m^2)	2.5	acres	
		MASS (weight)		
g	grams	0.035	ounces	oz
kg	kilograms	2.2	pounds	lb
t	tonnes (1000 kg)	1.1	short tons	
		VOLUME		
ml	milliliters	0.03	fluid ounces	fl oz
l	liters	2.1	pints	pt
l	liters	1.06	quarts	qt
l	liters	0.26	gallons	gal
m^3	cubic meters	35	cubic feet	ft^3
m^3	cubic meters	1.3	cubic yards	yd^3
		TEMPERATURE (exact)		
°C	Celsius temperature	9/5 (then add 32)	Fahrenheit temperature	°F

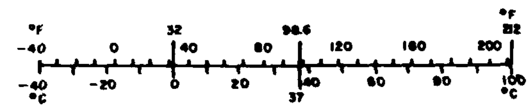

TABLE OF CONTENTS

LIST OF ILLUSTRATIONS

LIST OF TABLES

INTRODUCTION

PURPOSE.

The purpose of this experiment was to provide static and flight test data with the proposed Microwave Landing System (MLS) clearance format to support the MLS International Standards and Recommended Practices (SARPS) development by the International Civil Aviation Organization (ICAO) working group.

SYSTEM DESCRIPTION

GROUND SYSTEM/EQUIPMENT DESCRIPTION.

The Bendix Small Community (SC) Microwave Landing System Azimuth Subsystem without the monitor pole is shown in figure 1. A monitor pole was not used during the clearance assessment testing. The azimuth unit utilizes a Rotman lens which feeds 46 slotted waveguide elements spaced so as to form a vertical fan beam 3 degrees in width and 20 degrees in elevation, with a sharp underside cutoff. This antenna provides proportional guidance from left 10 degrees to right 10 degrees. Built-in sector antennas provide full fly-left and full fly-right coverage from 10 to 40 degrees. Similar antennas are used to provide identification (ID) and out-of-coverage indication (OCI) functions. Figure 2 indicates the azimuth coverage of each antenna.

THEORY OF OPERATION OF THE MLS AIRBORNE RECEIVER.

The MLS time reference scanning beam (TRSB) airborne receiver (figure 3) uses a dwell gate processor which envelope detects the "TO" or "FRO" scanning beam and applies a -3 decibels (db) beam threshold from which a dwell gate is generated. The midpoint time (t) is calculated from four dwell gate edge measurements (t_1, t_2, t_3, and t_4).

$$t_{TO} = \frac{1}{2}(t_1 + t_2)$$

$$t_{FRO} = \frac{1}{2}(t_3 + t_4)$$

$$t = t_{FRO} - t_{TO}$$

The angle estimate is then given by

$$\phi = \frac{1}{K}(t - t_o)$$

Where K = 0.10 ms/deg

t_o = 6.8 ms

In a standard right-handed rectangular coordinate system this angle is called a conical angle and is equivalent to:

$$\phi = \sin^{-1}\left(\frac{-Y}{\sqrt{X^2 + Y^2 + Z^2}}\right)$$

Where the azimuth unit is aimed along the +X axis.

In addition to computing an angle estimate, the receiver signal processor performs a critical function known as signal acquisition and validation. The signal acquisition process essentially involves making signal amplitude measurements; whereas, the measurements of signal quality involve a collection of time measurements.

The first event which must occur properly is the identification of the scan function; no beam functions are performed without a proper IDENT code.

The second function performed is to determine if the beams are stable and persistent. This is determined by comparing the amplitude of the signal inside the tracking gate with the amplitude of all signals outside the tracking point. For azimuth acquisition, a "confidence" counter must be incremented beyond a count of 14 before an unknown signal is declared the correct signal and the "confidence" flag is raised. Interruption of data for longer than 20 seconds will cause the confidence flag to drop.

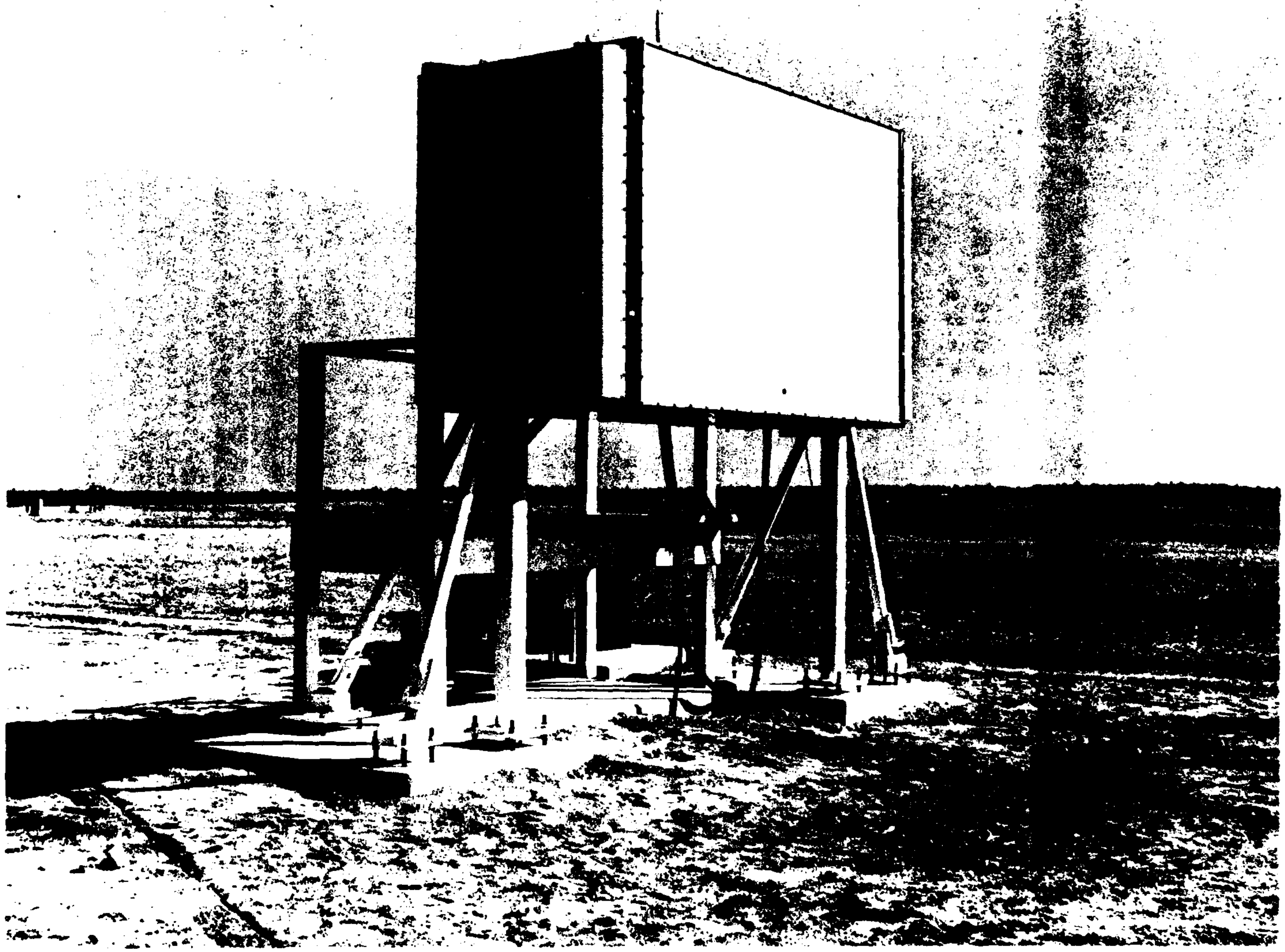

FIGURE 1. BENDIX SMALL COMMUNITY MICROWAVE LANDING SYSTEM AZIMUTH SUBSYSTEM

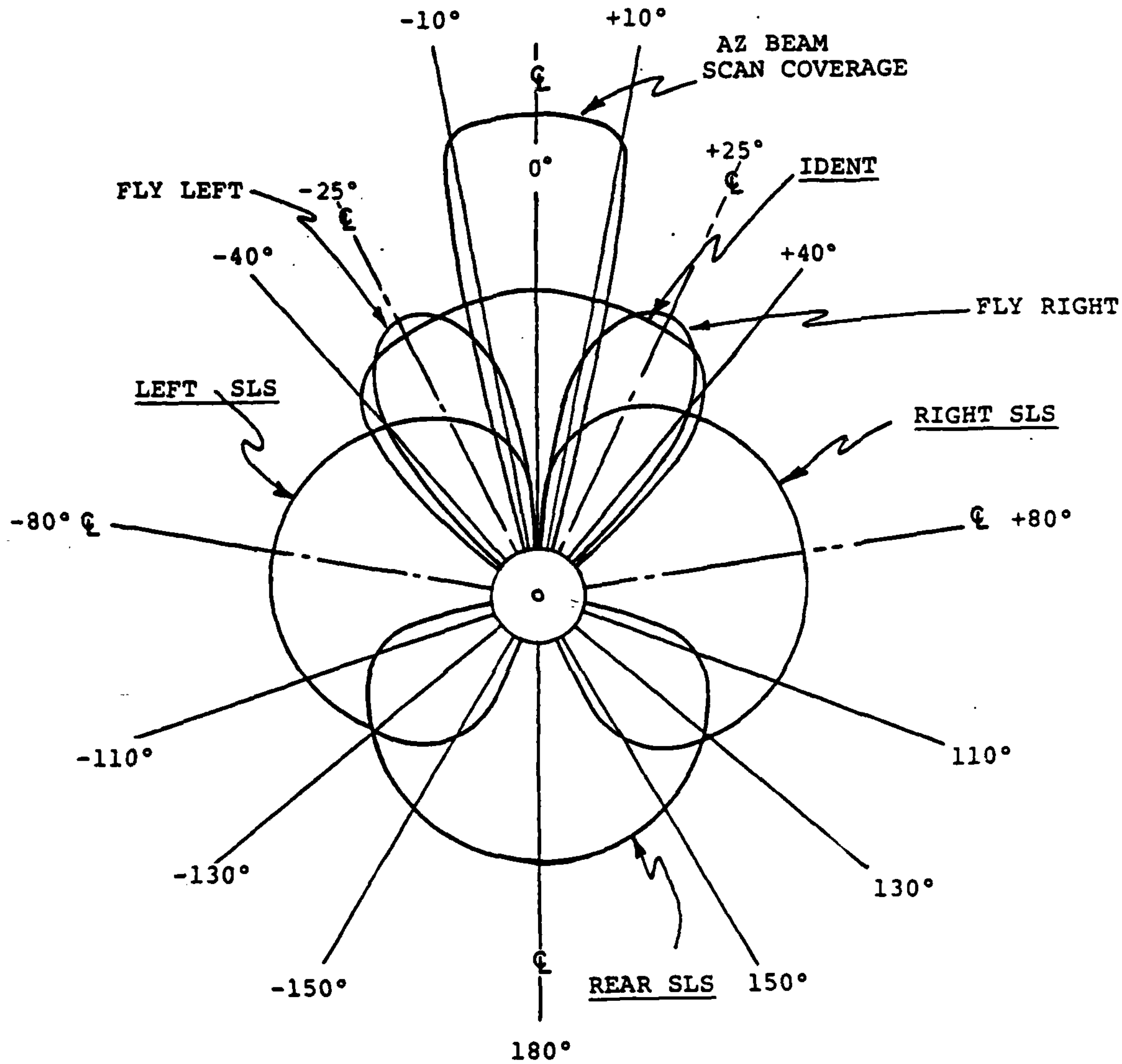

80-46-2

FIGURE 2. AZIMUTH COVERAGE

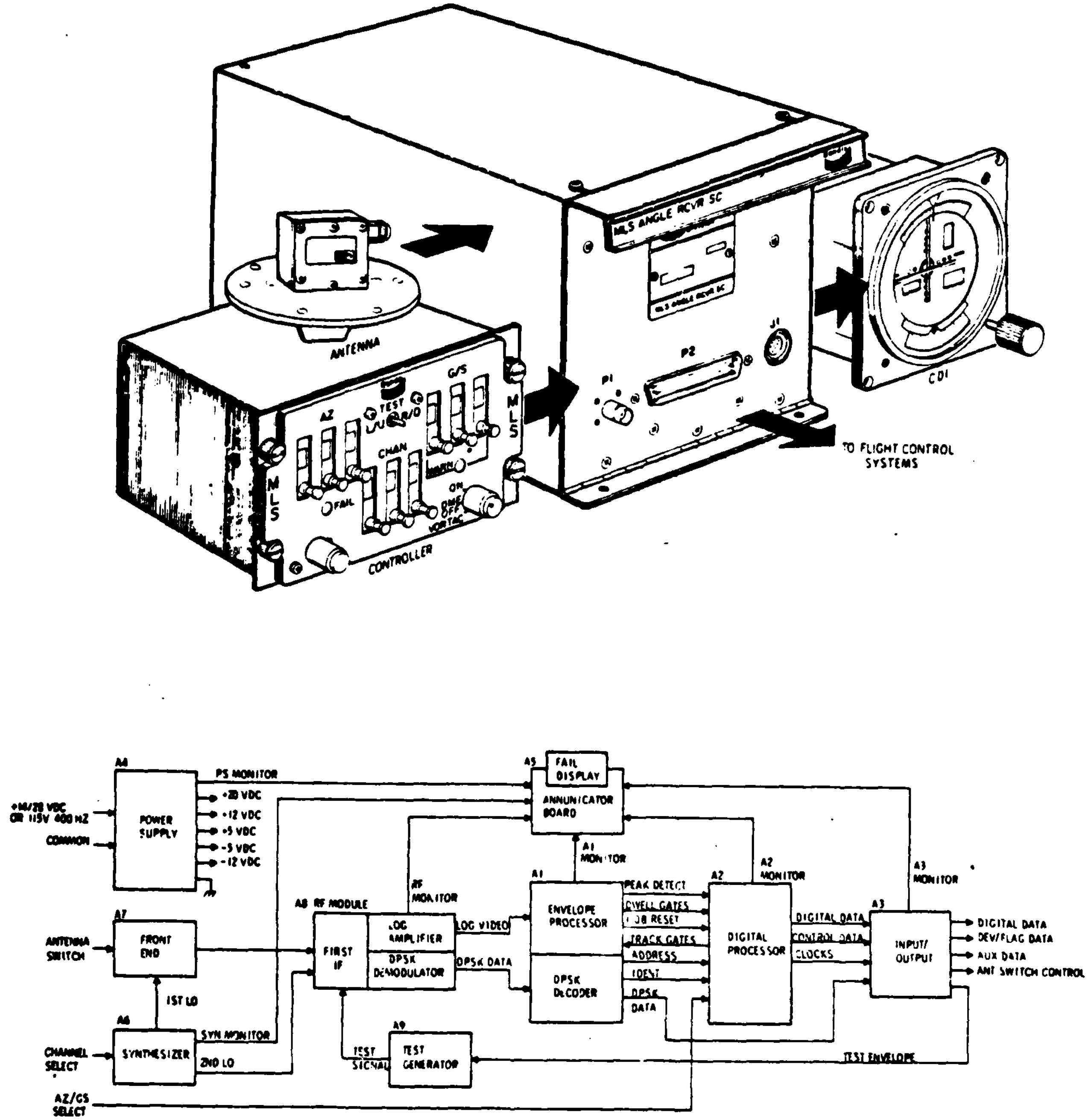

80-46-3

FIGURE 3. MLS ANGLE RECEIVER AND BLOCK DIAGRAM

The next process is to determine the quality of the signal which requires that the TO-FRO beams have the correct shapes and relative time positions. The criteria for the frame counter to be incremented by one are:

1. A valid identification must be decoded as part of the function preamble.

2. Only one pair of dwell gate edges must be present for each half scan.

3. The dwell gate width must be less than 350 microseconds (μs).

4. The dwell gate centroids must be symmetric about the midscan time within 125 μs.

5. The scanning beam amplitude must be greater than the out-of-coverage indication (OCI) signals.

When the frame counter exceeds seven counts for the azimuth function, the frame flag is raised. Interruption of data for longer than 1 second will cause the frame flag to drop.

When the frame flag and confidence flag are both up, the system flag is raised and the system switches to the track mode. If one of the data quality checks fail, the system then reverts to a coast mode, and the best estimate of the missing data point (or rejected data) is inserted in its place by an $\alpha - \beta$ tracker (recursive filter). An angle is considered bad if the rate of change of any MLS angle is greater than 1 degree/second. This filter provides three outputs: a smoothed angle, X_k; a prediction of the next filter input angle, Y_{k+1}; and a velocity term, V_k, which measures the rate of change of the input angle. The present raw data input angle is U_k; the predicted input from the previous scan is Y_k. The filter is summarized by the following three equations:

$$X_k = \alpha U_k + (1-\alpha)Y_k$$

$$V_k = \sum_{n=1}^{k} (U_n - Y_n)$$

$$Y_{k+1} = X_k + \beta V_k$$

k = Data sample index number
n = Sample size.

The constants for the azimuth signal are:

$$\alpha = 1/4$$

$$\beta = 1/32$$

A clearance counter is used to measure the reliability of data obtained from the right and left clearance pulses. The counter is incremented each time the magnitude of the CLR pulse is greater than the SLS peak and the SLS peak exceeds the scanning beam peaks. For good clearance data the count must exceed seven for azimuth. If the clearance flag is raised, the receiver enters the clearance mode and outputs the full-scale azimuth deviation to the course deviation indicator (CDI).

TEST CONFIGURATION.

The Bendix Small Community Azimuth equipment was modified by the contractor to generate the clearance signals as proposed by the All Weather Operations Panel (AWOP) representative from the United Kingdom (U.K.). Existing and proposed Small Community Azimuth formats are shown in figures 4 and 5, respectively. Two clearance signal shapes were evaluated. The first was a pulse resembling one-half of a 5.4 degree scanning beam, with the exact shape and one-half power width being dependent upon the traveling wave tube amplifier (TWTA) drive signal level. Figure 6 represents the approximate wave shape and pulse width. The second shape to be evaluated was a 35 μs square pulse.

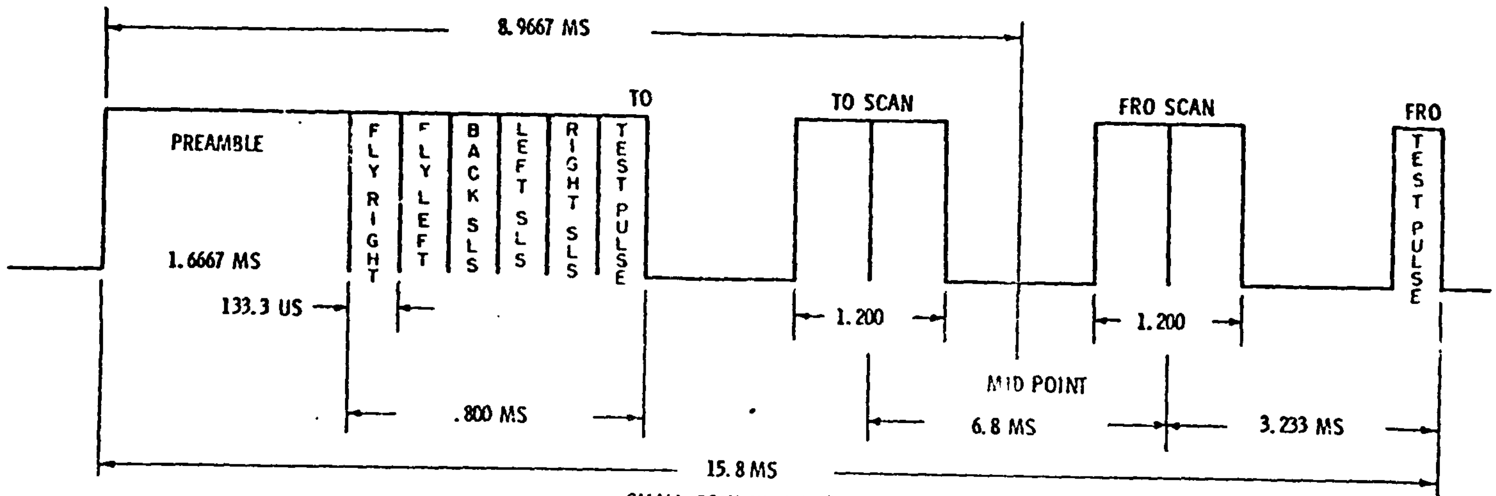

SMALL COMMUNITY AZIMUTH FORMAT

LENGTH OF PREAMBLE = 1.6667 MS

LENGTH RIGHT CLEARANCE, LEFT CLEARANCE, BACK, LEFT, RIGHT SLS, TO AND FRO TEST PULSES = 0.1333 MS

TO AND FRO SCANS = 1.200 MS

80-46-4

FIGURE 4. EXISTING SMALL COMMUNITY AZIMUTH FORMAT

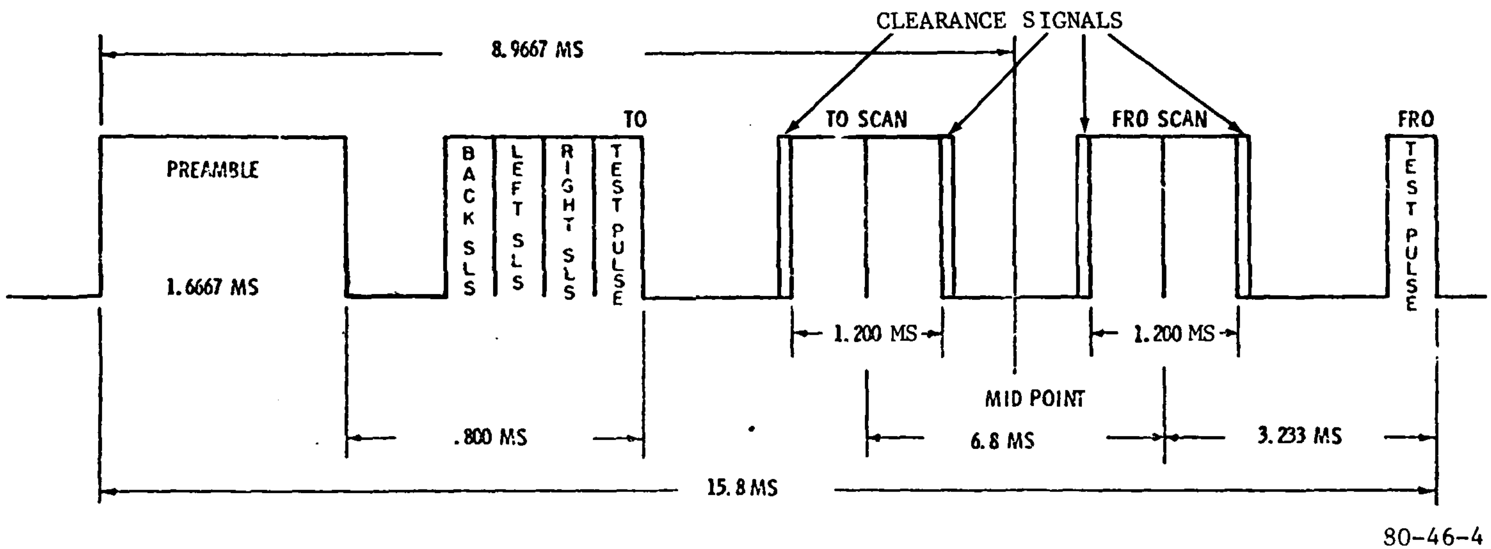

FIGURE 5. PROPOSED SMALL COMMUNITY AZIMUTH FORMAT

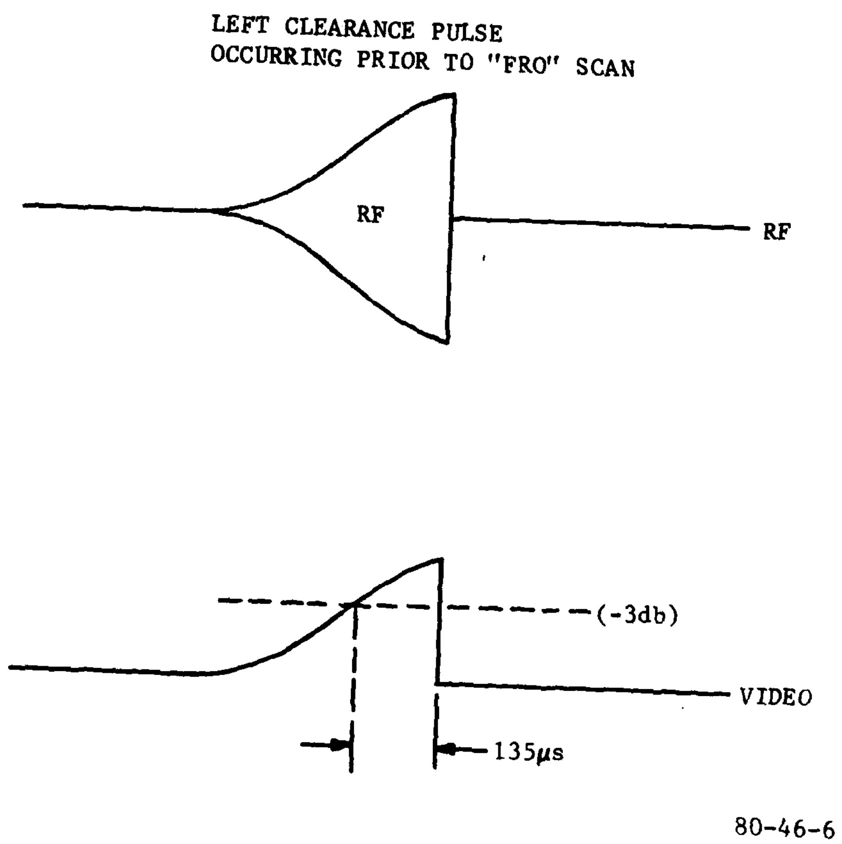

FIGURE 6. SHAPED PULSE

Each type of pulse was transmitted at the edge of proportional coverage. They were positioned in time to merge with the scanning beams at an angle of 12.462 degrees.

Additional modifications were made for certain test configurations. A radio-frequency (RF) phase shifter was inserted in the clearance antenna line to vary the relative RF phase relationship between the clearance and scanning beam signals. The attenuation or termination of certain functions was also necessary during some tests.

The SC MLS azimuth antenna was installed in two locations (figure 7) at the Federal Aviation Administration (FAA) Technical Center, Atlantic City Airport, New Jersey. A clean site (no obstructions) in the approach zone of runway 13 was the first to be utilized. Both static and flight data were collected at this site. A second location, behind the FAA hangar (bldg. 301), was also used for flight tests only. The large hangar structure provided an excellent reflector during the multipath flight testing. Figure 8 indicates the antenna position relative to the hangar and the azimuth boresite (0 degrees) direction.

TEST PROCEDURES AND RESULTS

STATIC TEST PROCEDURES.

Static data were collected using a mobile test van (figure 9), with a receiving antenna height of 50 feet above the ground level. A block diagram of the van instrumentation is shown in figure 10. A series of data points were used between the pure scanning beam signal region and the pure clearance signal region. Figure 11 shows the relationship of the test van to the azimuth ground station. Only the negative angle side was used due to airport vehicular restrictions and the convenience of an existing road.

The elevation angles, with respect to the azimuth antenna phase center, for most of the data points ranged between 1.0 and 0.96 degrees. The azimuth angles ranged between -10 and -17 degrees.

At each data point, the statistical data recorded included a mean angle, a standard deviation, a minimum angle, a maximum angle, and the number of frame flags. The system flag status was also recorded. In the absence of a system flag, the number of valid azimuth samples was 100. During a system flag condition no valid samples were available. If the receiver displayed an intermittant system flag, the data was considered unusable.

The receiver log video and dwell gates were observed during all the static tests. Tracking gates and filtered video (26 kilohertz (kHz) filter output) were also observed during some tests. Some video photographs were taken.

The receiver video photographs and a copy of the static data were provided to the MITRE Corporation representative, under contract to the Systems Research and Development Service (SRDS), who observed the static tests for SRDS.

During the first static test series, the ground system was radiating the shaped clearance signal. Two signal levels were used: clearance acquisition +3.0 dB and clearance acquisition +9.0 dB. Clearance acquisition was determined by positioning the test van in the pure clearance region, setting the test van attenuator to maximum, and then slowly decreasing the attentuation until the receiver acquired and held the clearance signal. The attenuation was then reduced further until the desired test ratio was reached.

Three clearance (CL) to scanning beams (SB) ratios were tested: -9, -4.5, and -3.0 dB. The CL/SB ratio was set by positioning the test van at an azimuth angle that produced a scanning beam dwell gate width of 75 μs (approximately

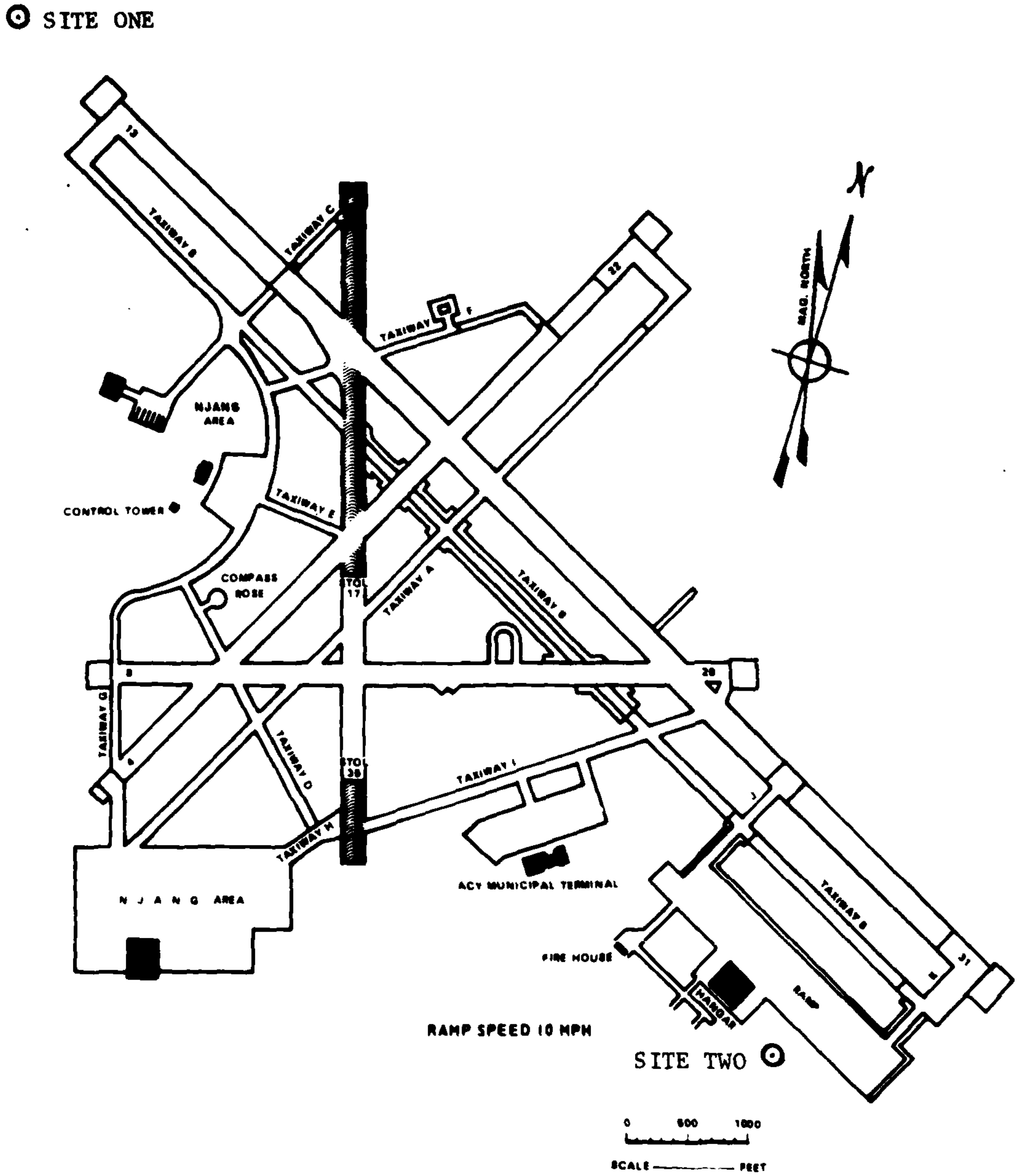

ATLANTIC CITY AIRPORT, ATLANTIC CITY, NEW JERSEY

80-46-7

FIGURE 7. SITE LOCATIONS

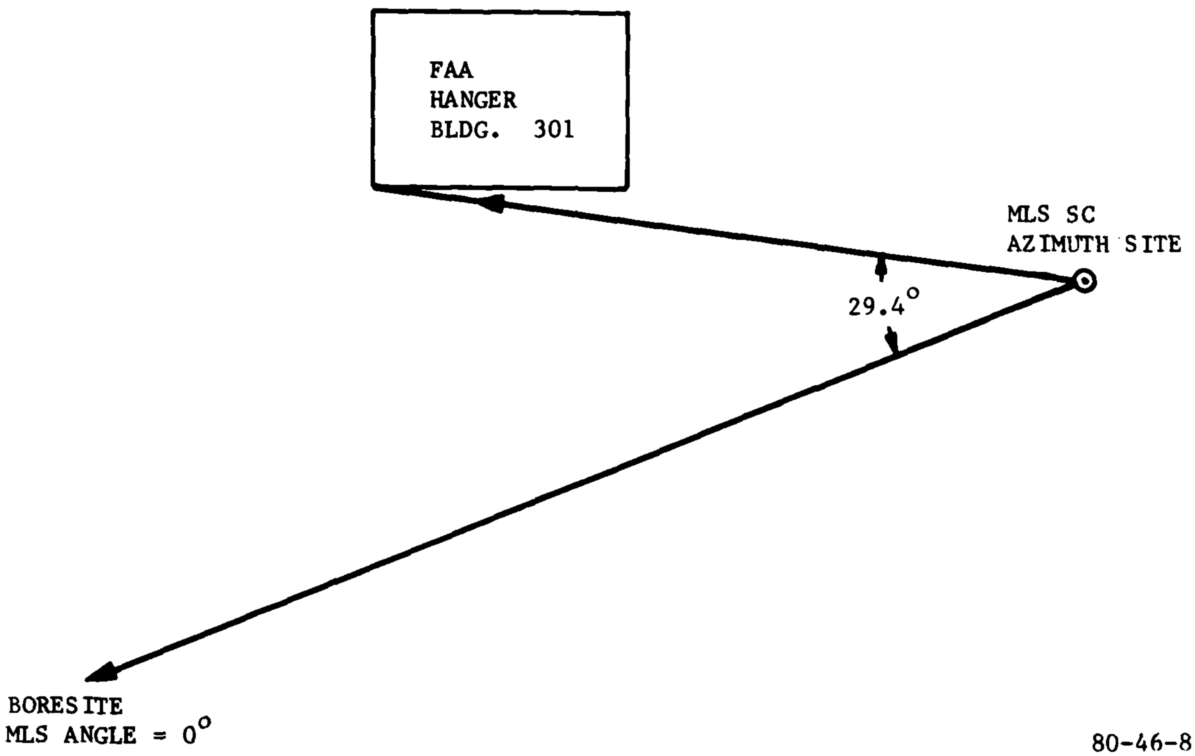

FIGURE 8. SITE 2 (HANGAR) ORIENTATION

FIGURE 9. MLS TEST VAN

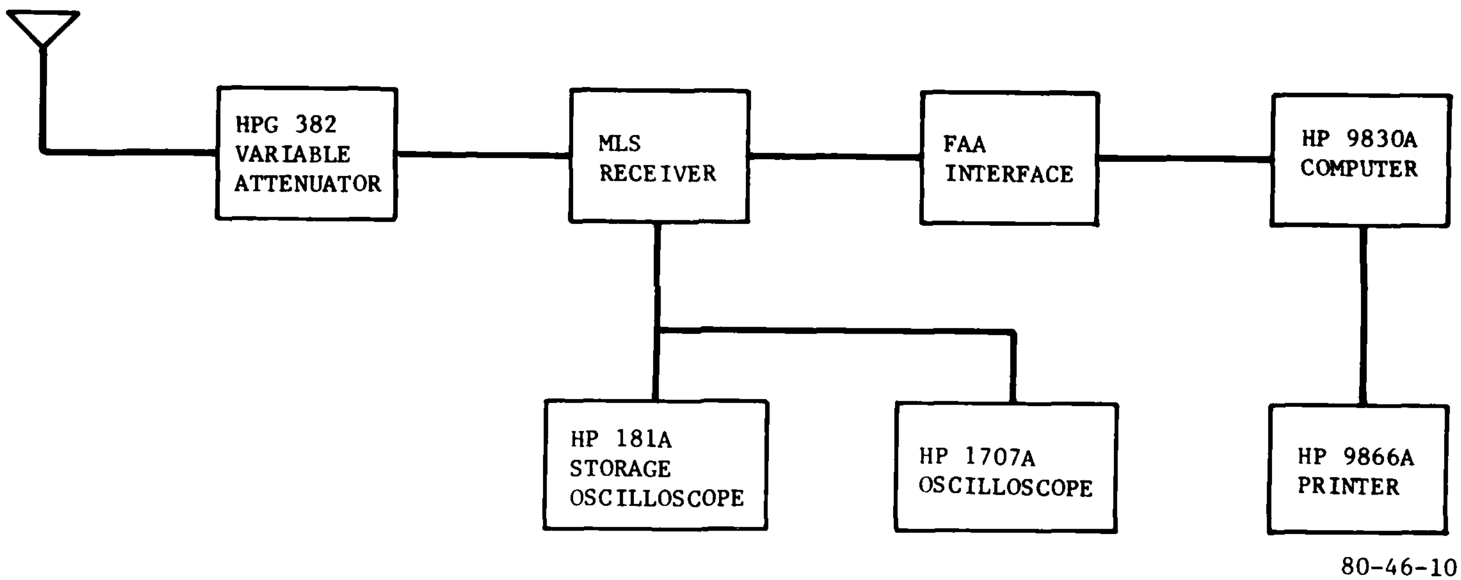

FIGURE 10. MLS TEST VAN DATA COLLECTION PACKAGE BLOCK DIAGRAM

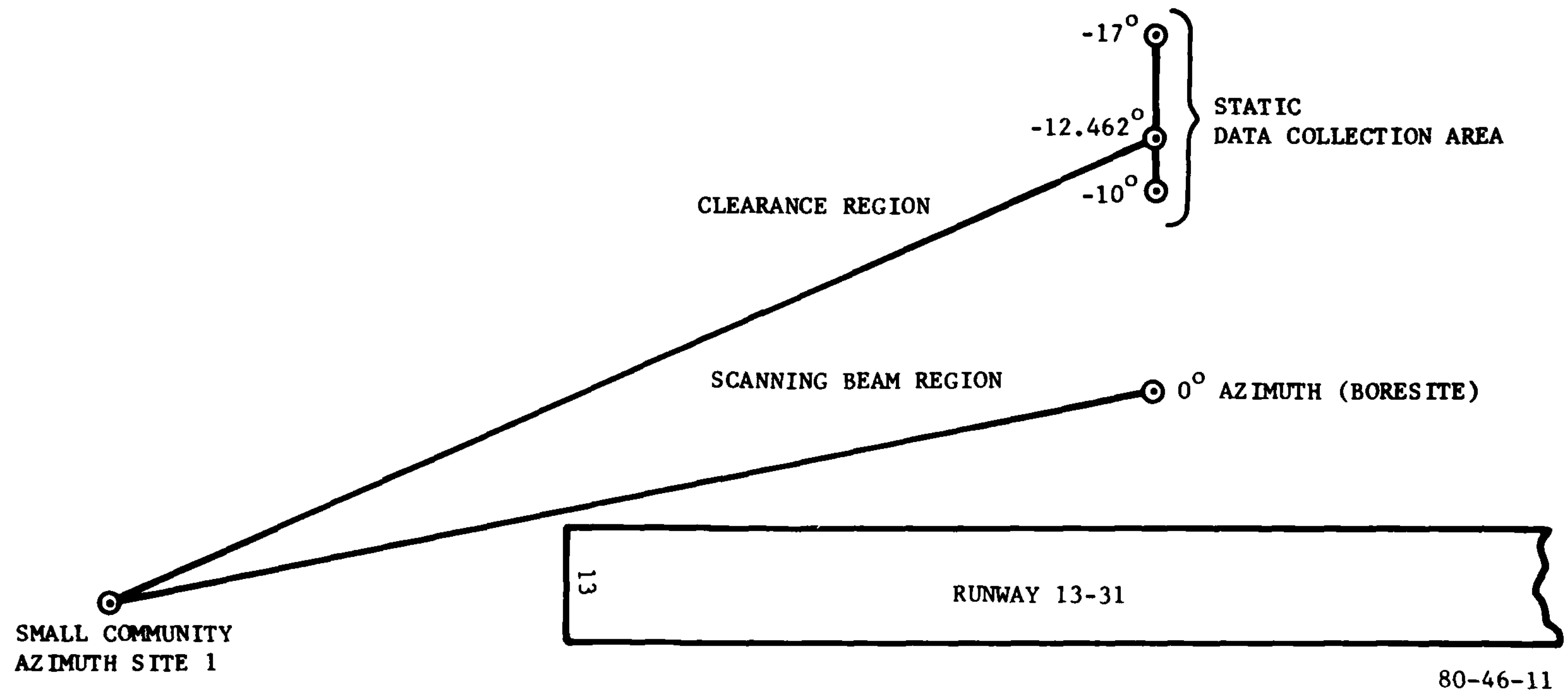

FIGURE 11. SITE 1 (RUNWAY) ORIENTATION

12.5 degrees) and reducing the scanning beam level until the desired ratio was obtained. For this portion of the test a CL/SB ratio of -4.5 dB at a CL acquisition level of +9 dB was investigated, at MITRE's request, for correlation with Calspan Laboratory simulations.

For the second static test series, the 35 μs square pulse was transmitted. The signal levels tested were clearance acquisition +3 dB and clearance acquisition +9 dB. The clearance to scanning beam ratios were CL/SB = -3 dB and CL/SB = -9 dB.

During all static testing and at each data point three sets of statistical data were taken. The first was with 180 degrees received RF phase shift between the clearance and the scanning beam signals, the second was with 0 degrees phase difference, and the third was with a varying phase relationship. Phase shifts were accomplished by inserting a four bit RF phase shifter in the clearance antenna line. At each data point the phase shifter was manually adjusted to produce 180 degree phase difference between the received SB and CL signals, as indicated by the deepest transition null in the log video, and then to 0 degree phase difference. For the varying phase condition, the shifter was clocked sequentially through its 16 phase increments. A summary of test conditions is contained in table 1.

STATIC TEST RESULTS.

The first test series (shaped pulse) showed poor results at the lower signal level using the existing Bendix MLS receiver. As described earlier, the receiver utilizes a multiple dwell gate test; more than one pair of dwell gates will decrement the frame counter. When the frame counter reaches zero, the frame flag drops causing a system flag. The slow rise (or fall) time associated with the shaped pulse and small noise perturbations caused multiple threshold crossings. This problem was accentuated by the reduced TWTA drive necessary to create the desired wave shape. Since the clearance signal level was reduced, it was necessary to terminate the OCI signals to prevent the receiver from flagging when the clearance or scanning beam level fell below the OCI level.

TABLE 1. STATIC TEST SUMMARY

Date	Clearance To Scanning Beam Ratio (dB)	Signal Level (dB Above Acquisition)	Clearance Pulse Type
2/8/80	-4.5	9	Shaped
2/14/80	-3	9	Shaped
	-9	9	
2/15/80	-3	3	Shaped
	-9	3	
2/22/80	-3	9	35 μs
	-9	9	
2/26/80	-3	3	35 μs
	-9	3	

Figure 12 are plots of calculated azimuth angle versus the receiver azimuth angle output and valid azimuth frame percentages using the shaped clearance pulse.

An acquisition test was done to determine the difference in receiver performance using the standard 3 degree scanning beam compared with the shaped clearance pulse. The receiver was placed in the pure scanning beam region with the clearance and OCI signals terminated. The SB signal level was then reduced below the receiver noise level, but still maintaining a function identification decode rate of 100 percent. As the SB signal was increased in small increments, the point at which the receiver acquired and held the SB was recorded. A similar procedure was utilized in the pure clearance region, except that this time the clearance signal was radiated and the scanning beam was terminated. It required approximately 3 dB more signal level to acquire and hold the shaped clearance pulse than it did the 3 degree scanning beam.

Since this condition made a fair evaluation of the proposed format difficult at low signal levels, an alternate clearance signal (a 35 μs square pulse) was chosen as a second test condition. It was wide enough to pass through the receiver without appreciable distortion, and narrow enough to minimize the multiple crossing problem associated with its flat top. A second acquisition test showed no preference between SB and CL signals.

During the second test series, the 35 μs square pulse exhibited better low signal performance than the wider shaped one. Figure 13 are plots of calculated azimuth angle versus the receiver azimuth angle, with an additional graph indicating the percentage of valid azimuth frames. Performance was as expected and no unusual results were found. Areas of system flag or poor performance were attributed to the multiple dwell gate problem described previously.

One system flag area was between -10.5 and 11.2 degrees true azimuth when the clearance to scanning beam (CL/SB) ratio was -3 dB (figures 13-g through 13-l).

When the CL/SB ratio was at this level, which also corresponds to the receiver dwell gate threshold point, a valid frame percentage of less then 100 occured over a large area between -10.5 and -15.5 degrees. A second system flag region between -14.8 and -15.2 degrees with the CL/SB ratio equal to -9 dB was also noted (figure 13-c). Although the only system flagged data occurred when the phase shift was equal to 180 degrees, the valid frame percentage dropped below 100 at one or more points between 14.3 and 17 degrees true azimuth angle (figures 13-a through 13-f).

FLIGHT TEST PROCEDURES.

An Aerocommander (N-50) was the FAA test aircraft. Figure 14 is a block diagram of the airborne data collection package. A modified MLS receiver was installed in the number one position in order to provide signal amplitude information as a part of the digital output data. Figures 15 and 16 are laboratory calibrations of receivers SC101 and SC103, respectively, and indicate the digital output number (a measure of signal amplitude) for a specific signal level input at the receiver RF input connector.

Aircraft space position was determined by the Nike-Hercules tracking facility. Azimuth, elevation, and range, with respect to the MLS SC azimuth antenna, were computed by the tracking facility and then telemetered to the test aircraft. This information, along with time, DME range, MLS azimuth angle, and the signal amplitudes of the preamble (ID), right clearance, left clearance, left out of coverage indication (OCI), rear OCI, right OCI, and "TO" and "FRO" beams were recorded digitally on the Kennedy 9800 tape unit. Analog deviation and flag signals were recorded on the brush 220 strip chart recorder.

The digital tapes were checked for quality and then forwarded, along with a receiver calibration, to Vitro for further processing. SRDS contracted with Vitro to provide data plots showing the signal amplitudes of the various functions versus the aircraft position. The analog strip chart recordings were used to check any abnormalities during the flight.

FLIGHT TEST RESULTS.

No attempt was made to analyze the airborne digital data at the Technical Center since the data tapes were sent to Vitro for processing immediately after a "quick look" check of the recorded data was performed. A Flight Test Summary is contained in table 2.

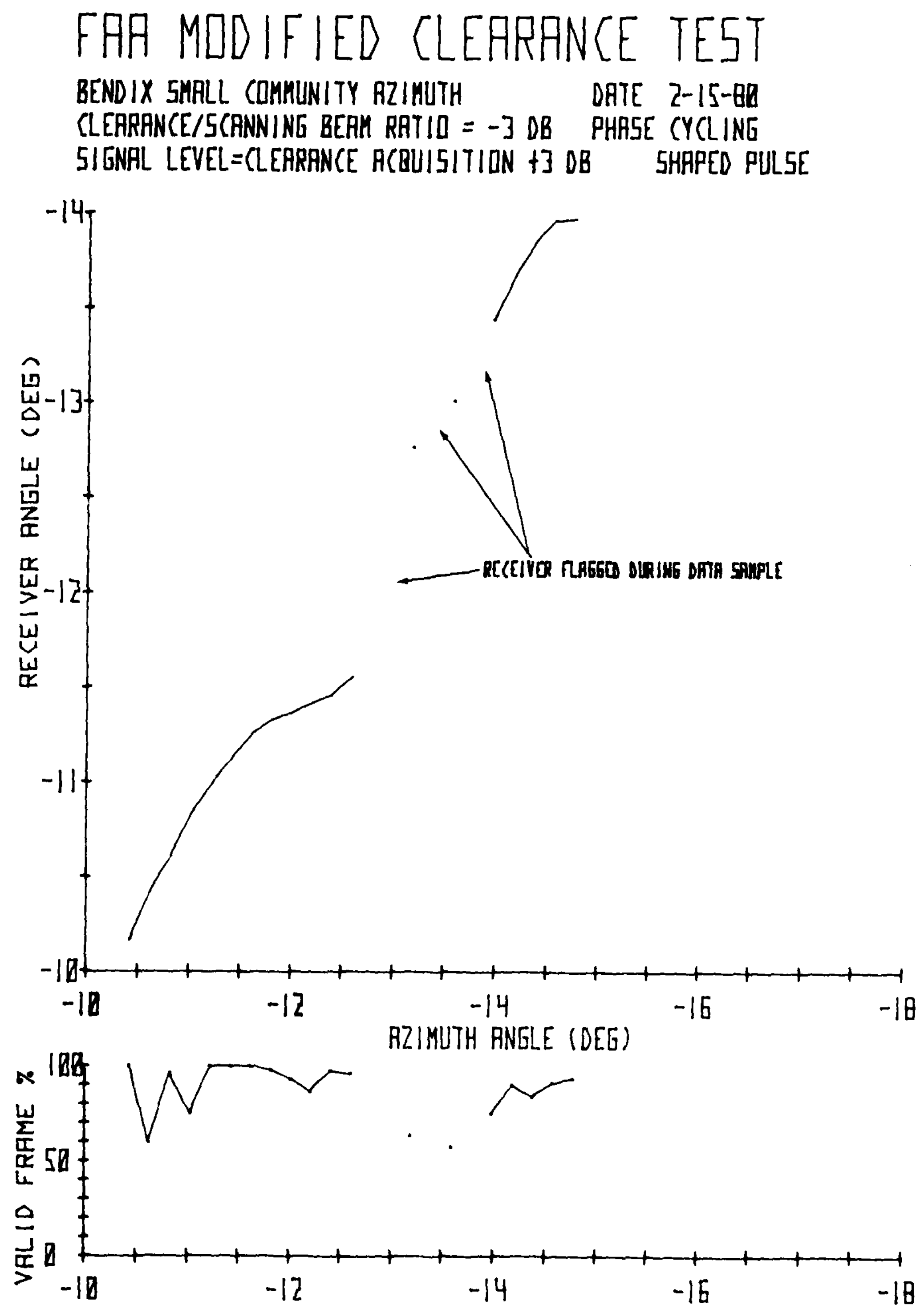

(a)

80-46-12-a

FIGURE 12. AZIMUTH RECEIVER ANGLE VERSUS TRUE AZIMUTH PLOTS USING THE SHAPED CLEARANCE PULSE (SHEET 1 OF 15)

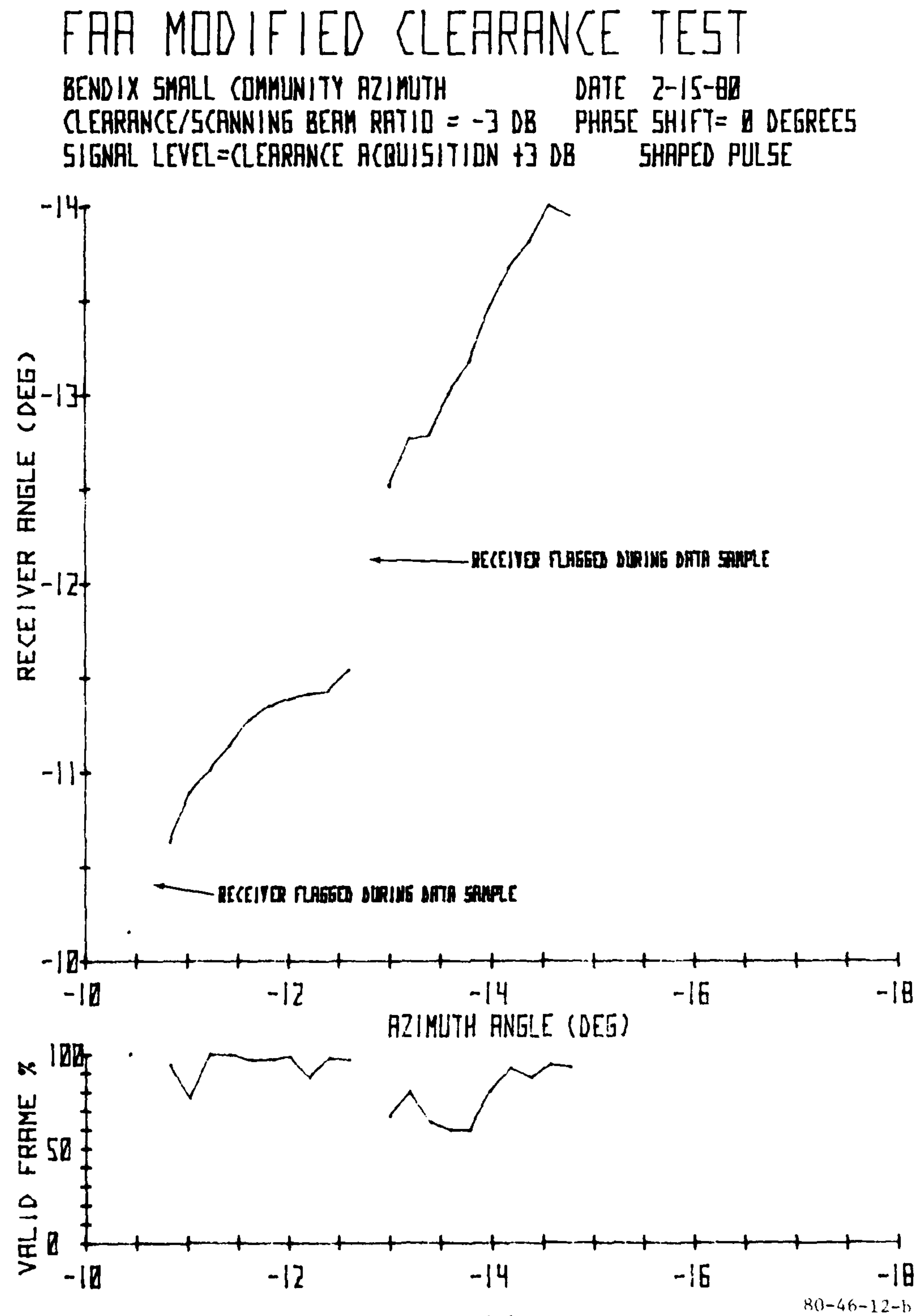

(b)

FIGURE 12. AZIMUTH RECEIVER ANGLE VERSUS TRUE AZIMUTH PLOTS USING THE SHAPED CLEARANCE PULSE (SHEET 2 OF 15)

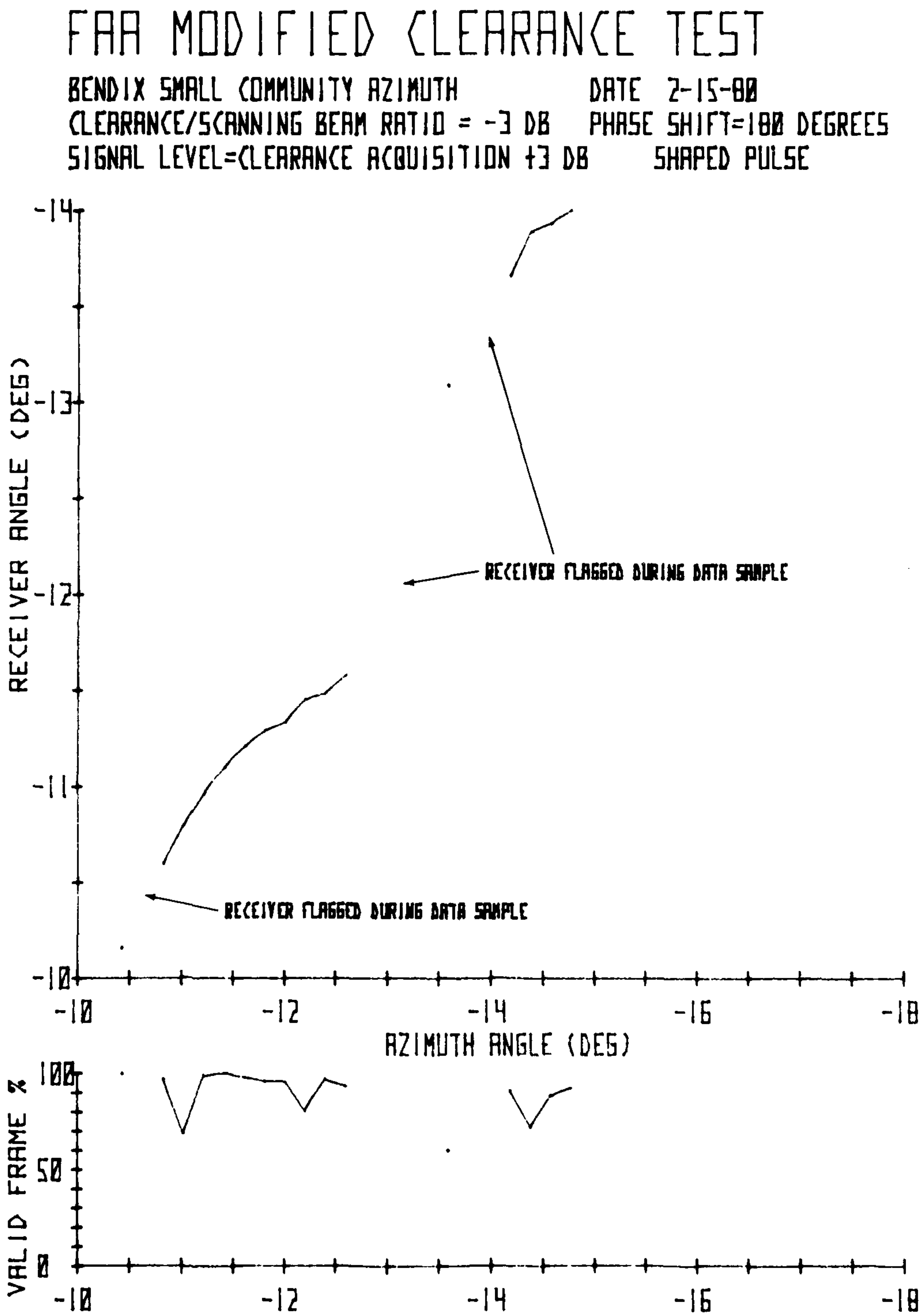

(c)

80-46-12-c

FIGURE 12. AZIMUTH RECEIVER ANGLE VERSUS TRUE AZIMUTH PLOTS USING THE SHAPED CLEARANCE PULSE (SHEET 3 OF 15)

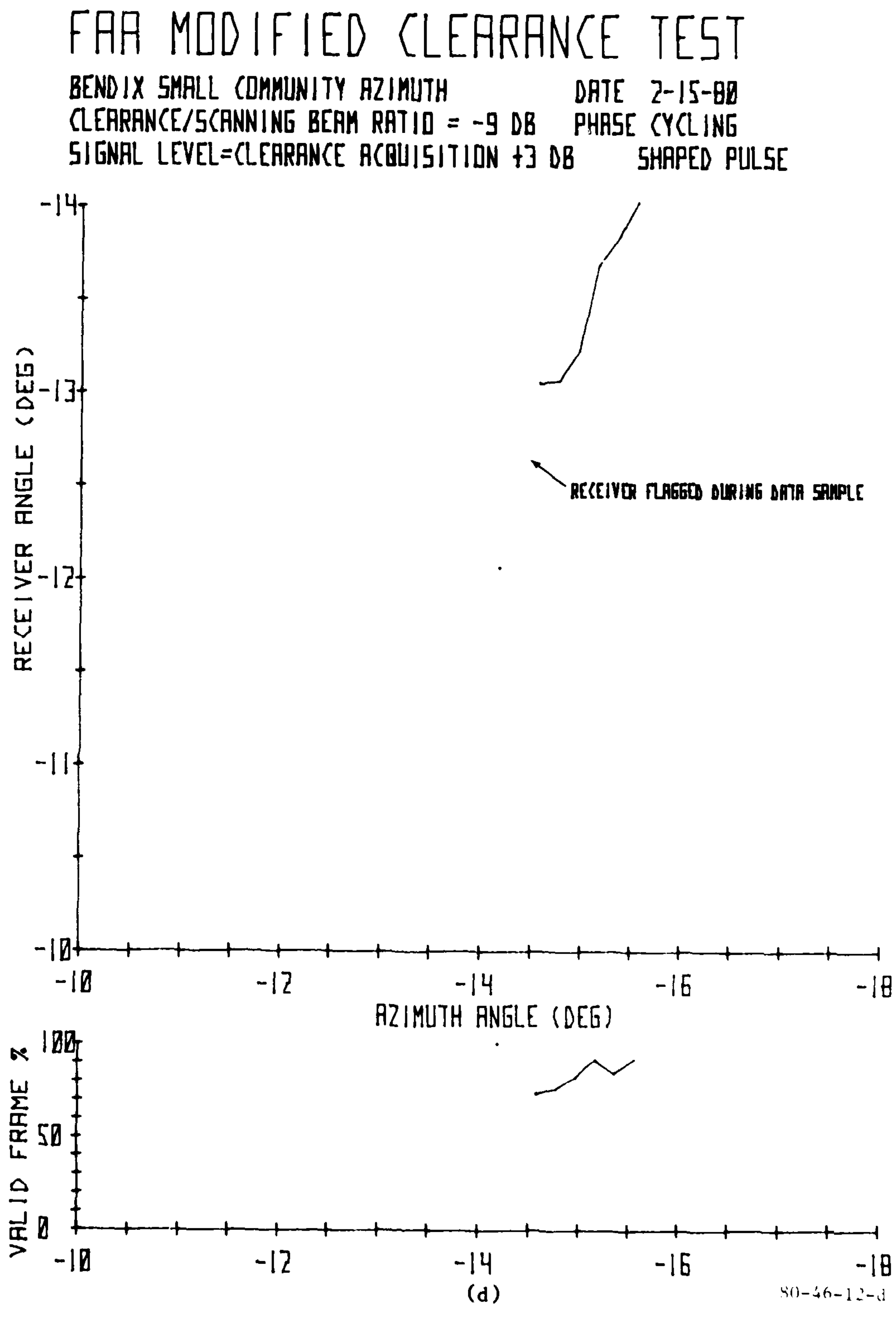

FIGURE 12. AZIMUTH RECEIVER ANGLE VERSUS TRUE AZIMUTH PLOTS USING THE SHAPED CLEARANCE PULSE (SHEET 4 OF 15)

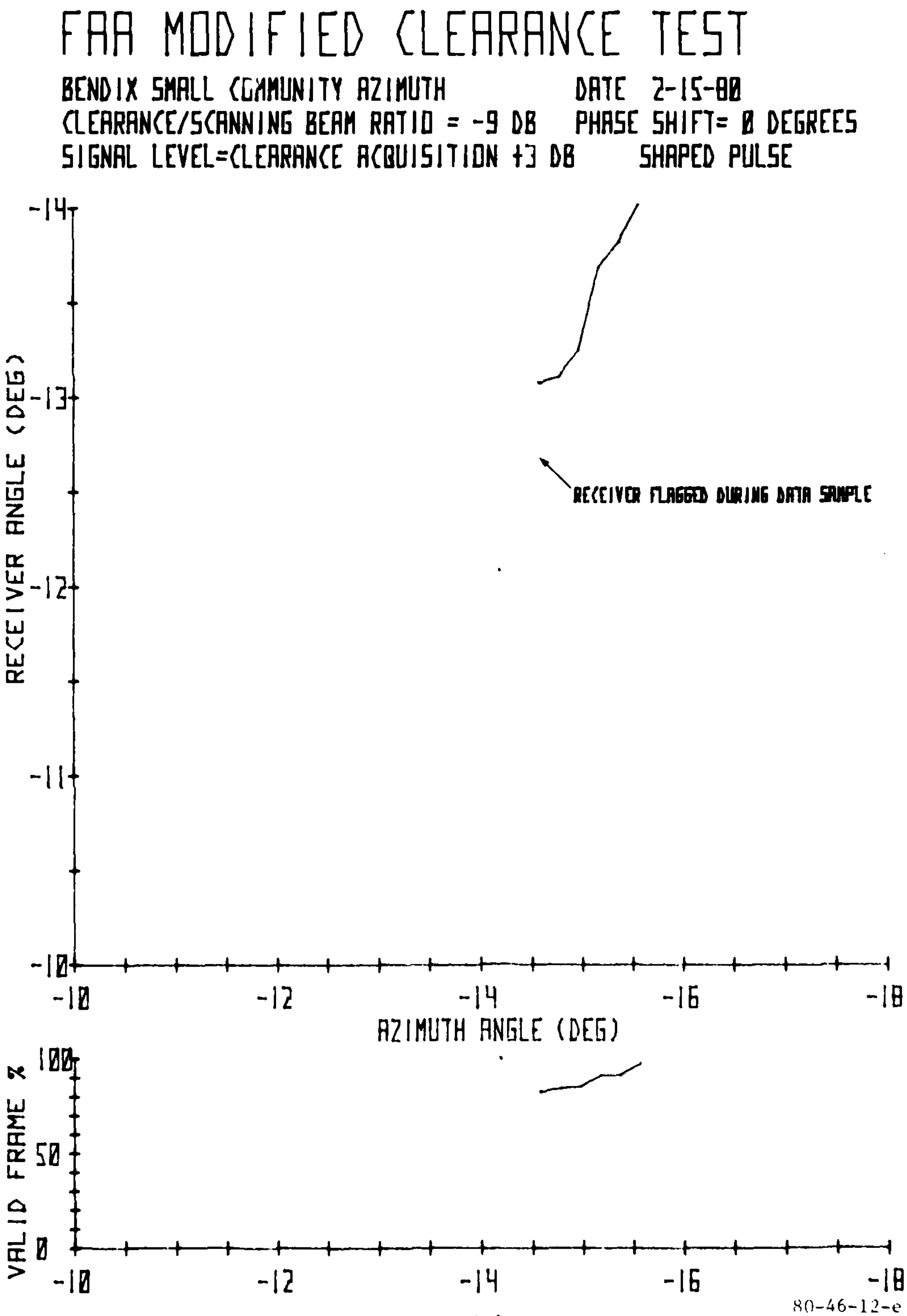

(e)

FIGURE 12. AZIMUTH RECEIVER ANGLE VERSUS TRUE AZIMUTH PLOTS USING THE SHAPED CLEARANCE PULSE (SHEET 5 OF 15)

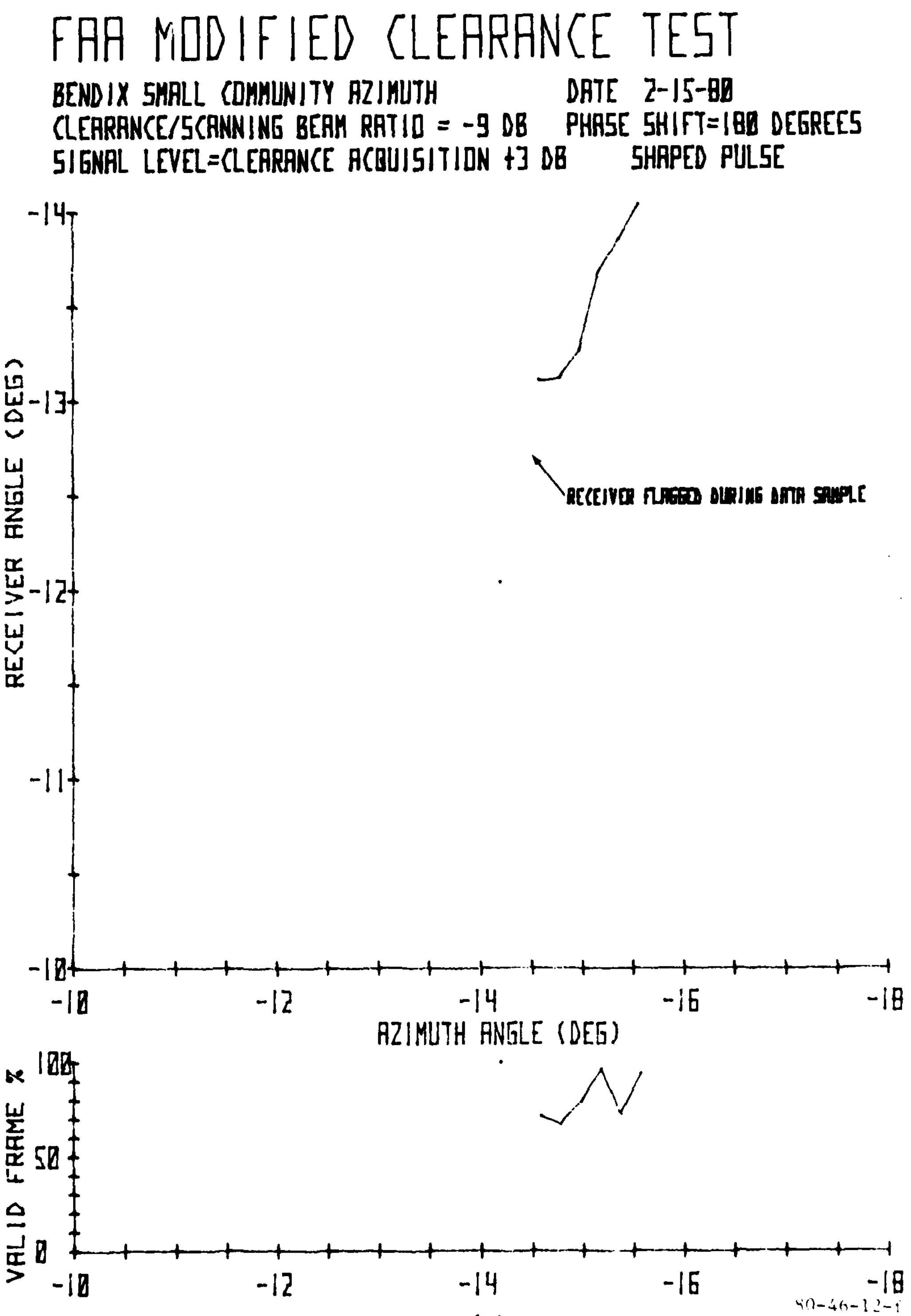

(f)

FIGURE 12. AZIMUTH RECEIVER ANGLE VERSUS TRUE AZIMUTH PLOTS USING THE SHAPED CLEARANCE PULSE (SHEET 6 OF 15)

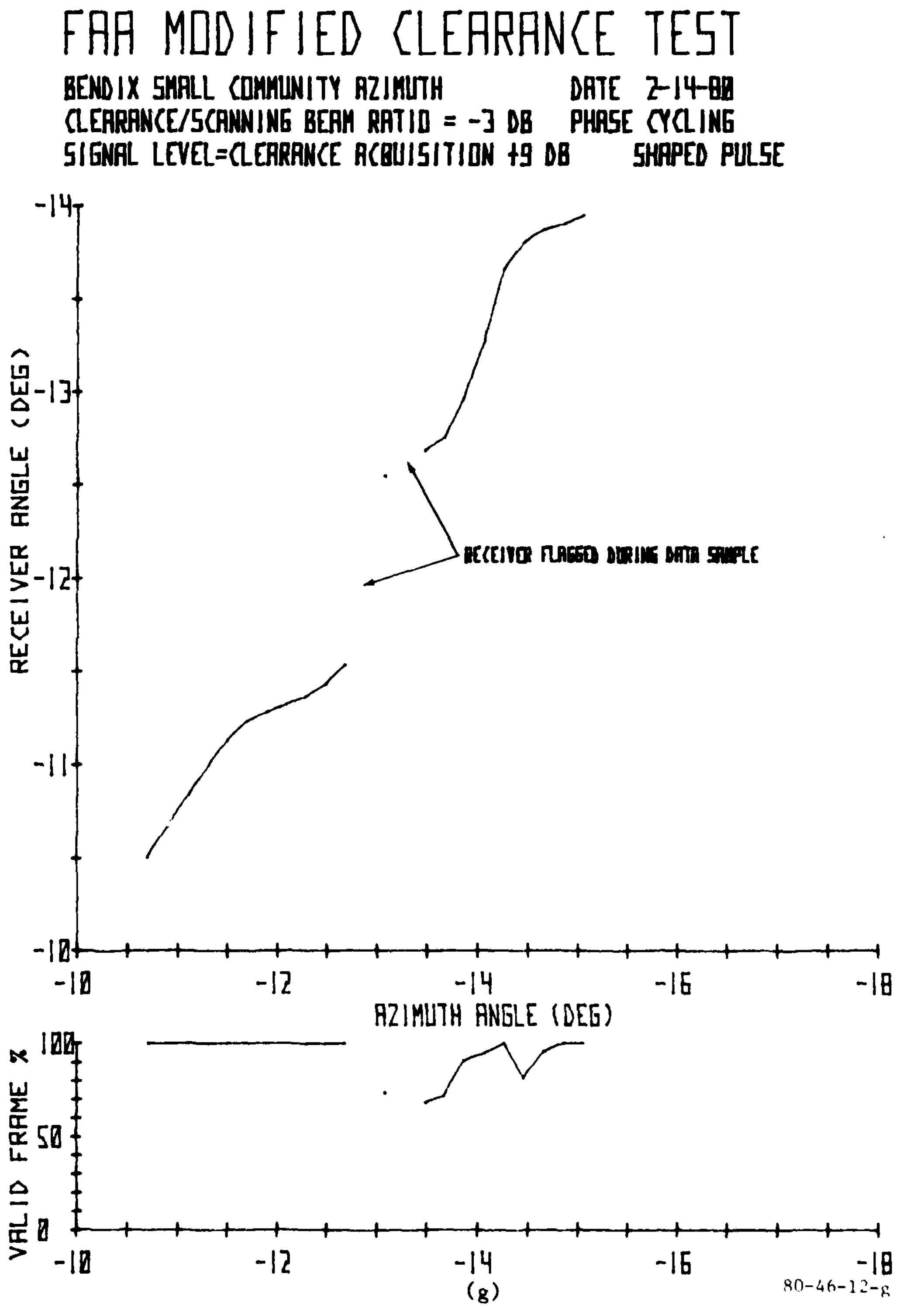

FIGURE 12. AZIMUTH RECEIVER ANGLE VERSUS TRUE AZIMUTH PLOTS USING THE SHAPED CLEARANCE PULSE (SHEET 7 OF 15)

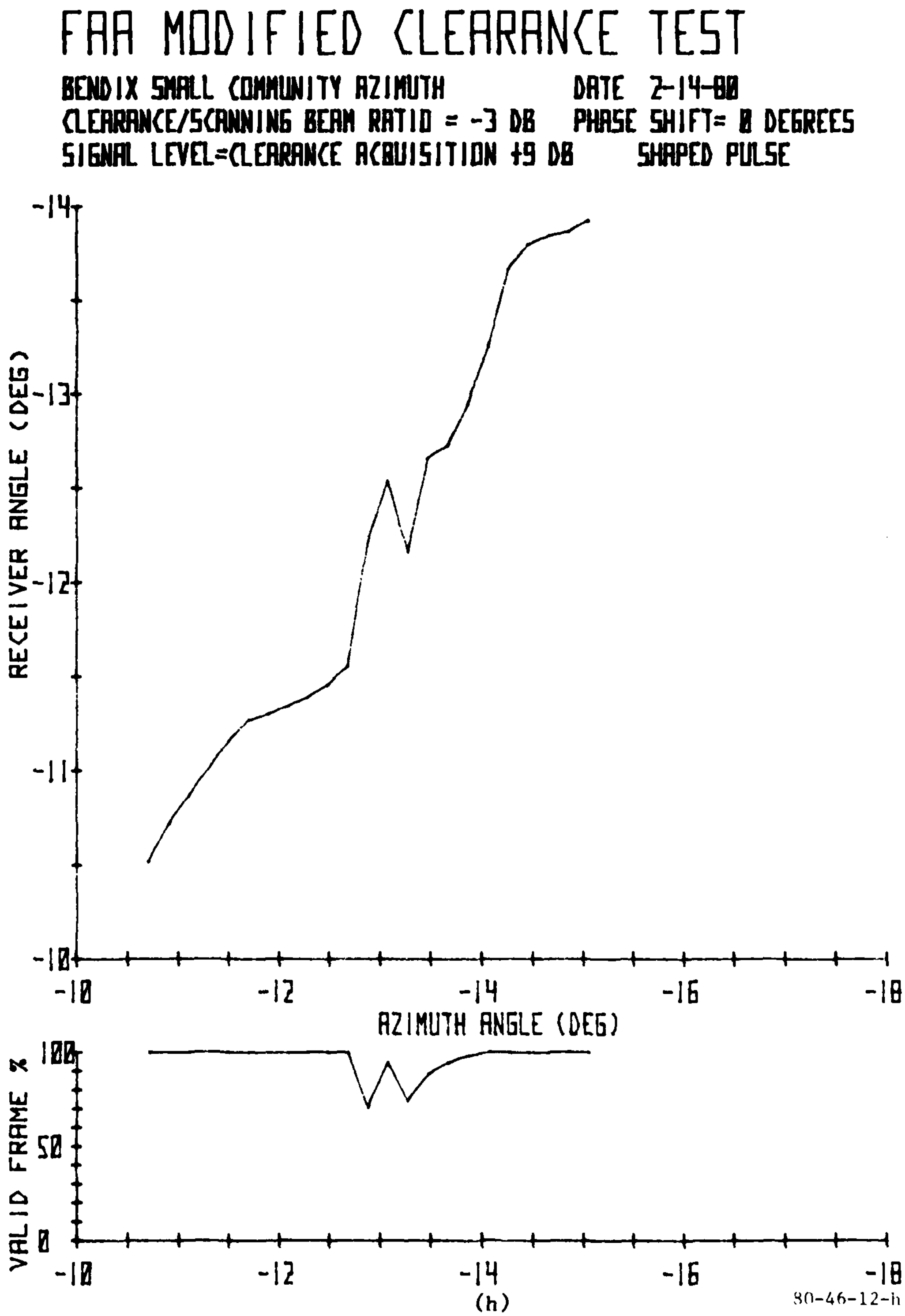

FIGURE 12. AZIMUTH RECEIVER ANGLE VERSUS TRUE AZIMUTH PLOTS USING THE SHAPED CLEARANCE PULSE (SHEET 8 OF 15)

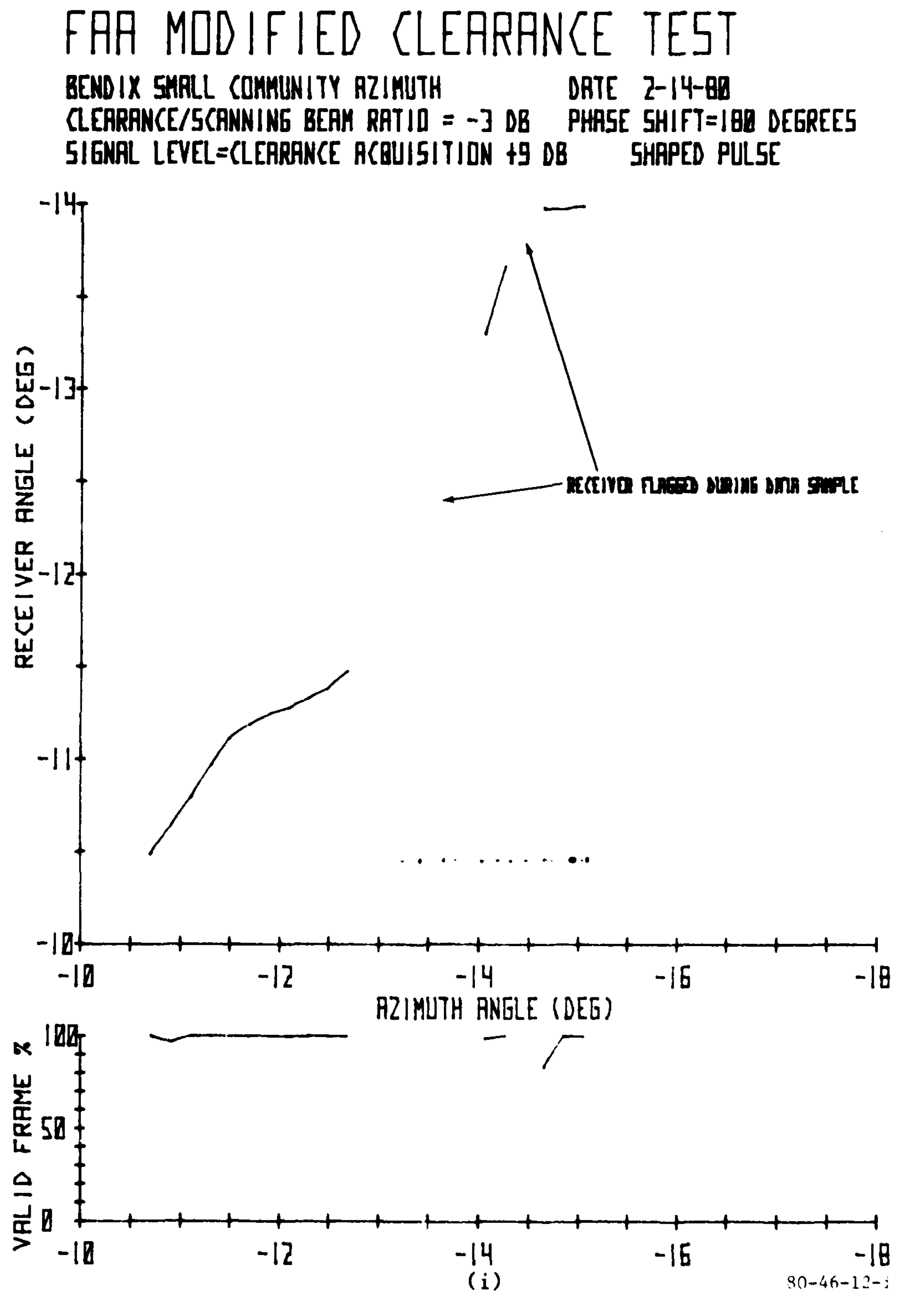

FIGURE 12. AZIMUTH RECEIVER ANGLE VERSUS TRUE AZIMUTH PLOTS USING THE SHAPED CLEARANCE PULSE (SHEET 9 OF 15)

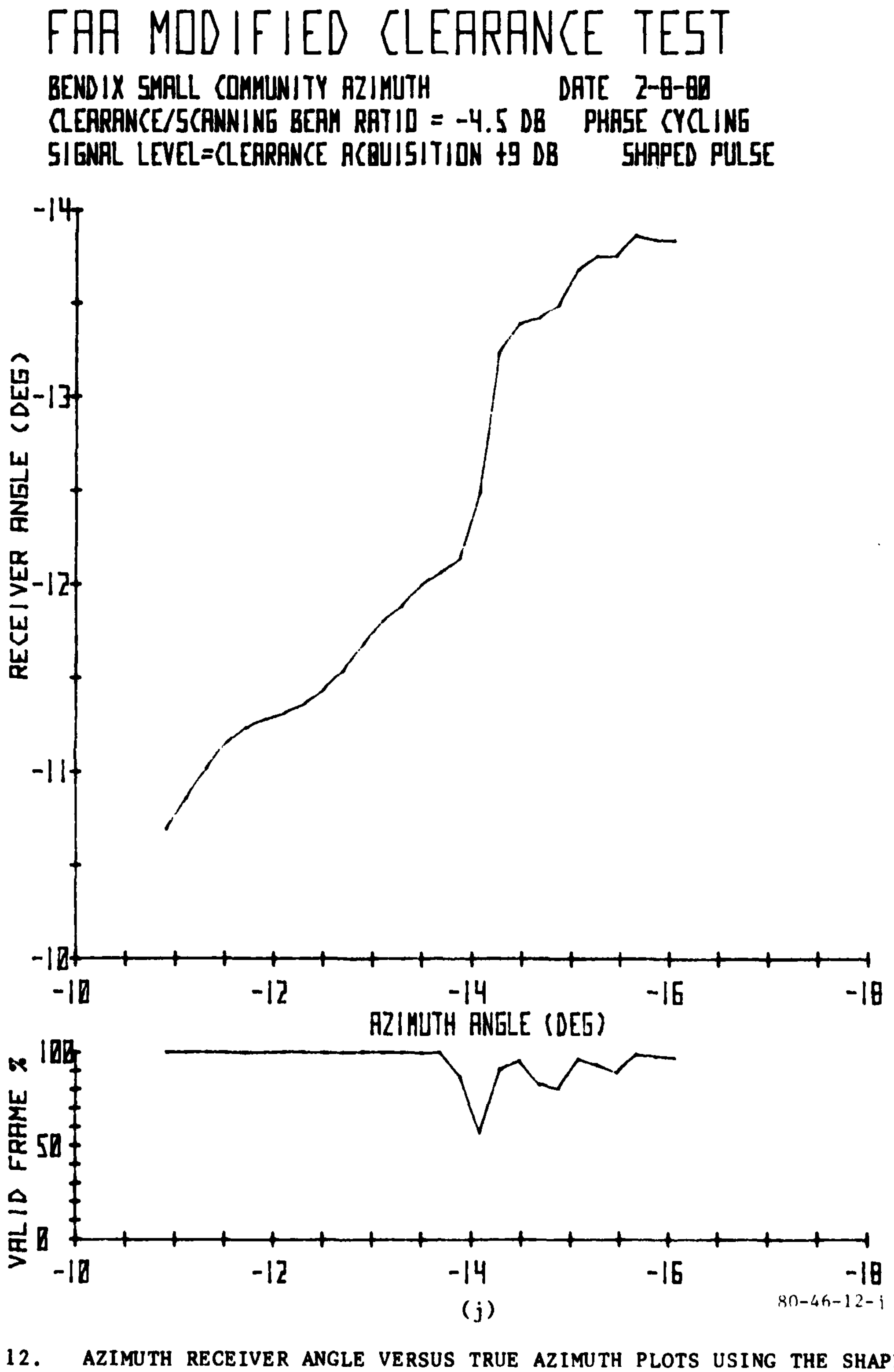

FIGURE 12. AZIMUTH RECEIVER ANGLE VERSUS TRUE AZIMUTH PLOTS USING THE SHAPED CLEARANCE PULSE (SHEET 10 OF 15)

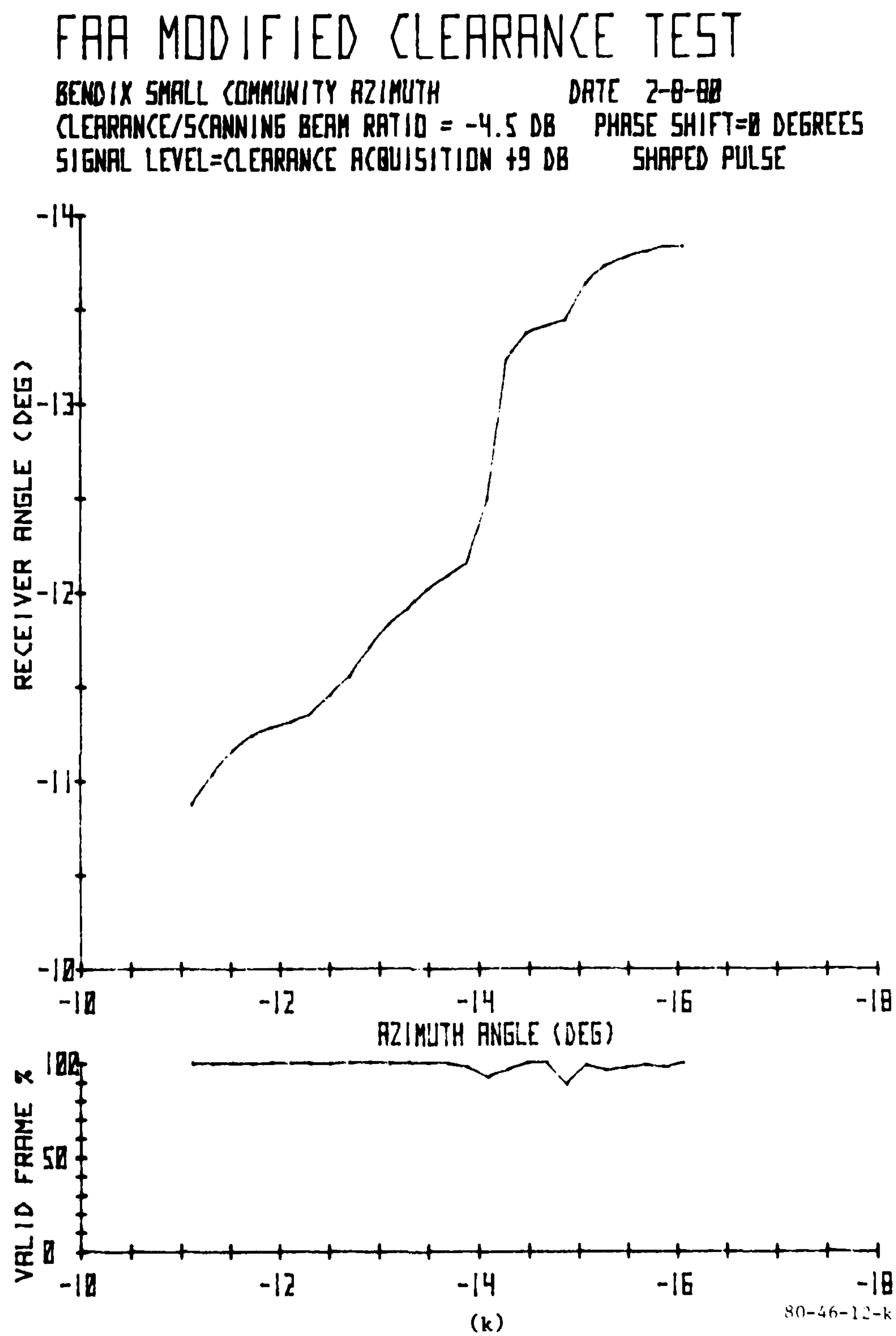

FIGURE 12. AZIMUTH RECEIVER ANGLE VERSUS TRUE AZIMUTH PLOTS USING THE SHAPED CLEARANCE PULSE (SHEET 11 OF 15)

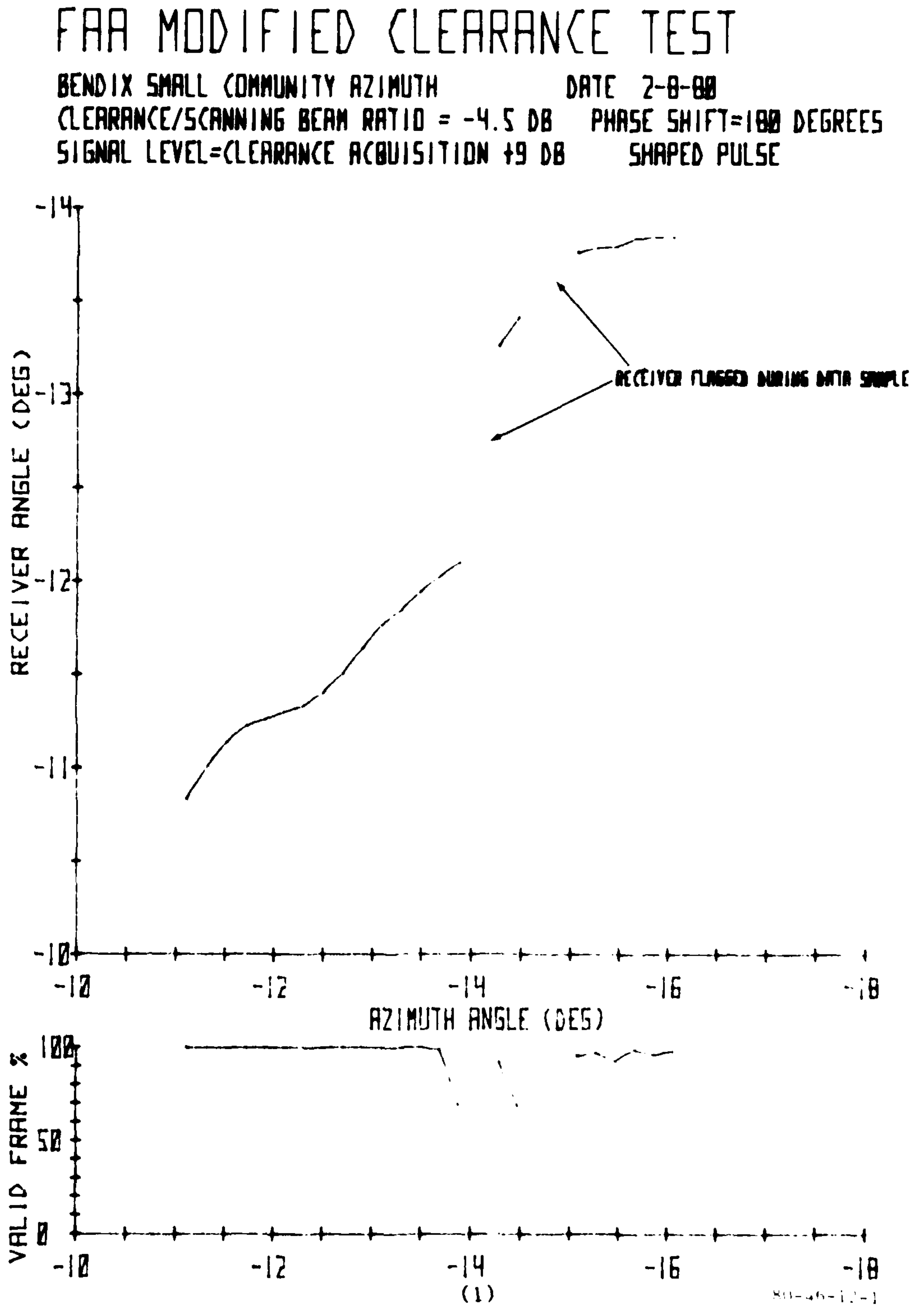

FIGURE 12. AZIMUTH RECEIVER ANGLE VERSUS TRUE AZIMUTH PLOTS USING THE SHAPED CLEARANCE PULSE (SHEET 12 OF 15)

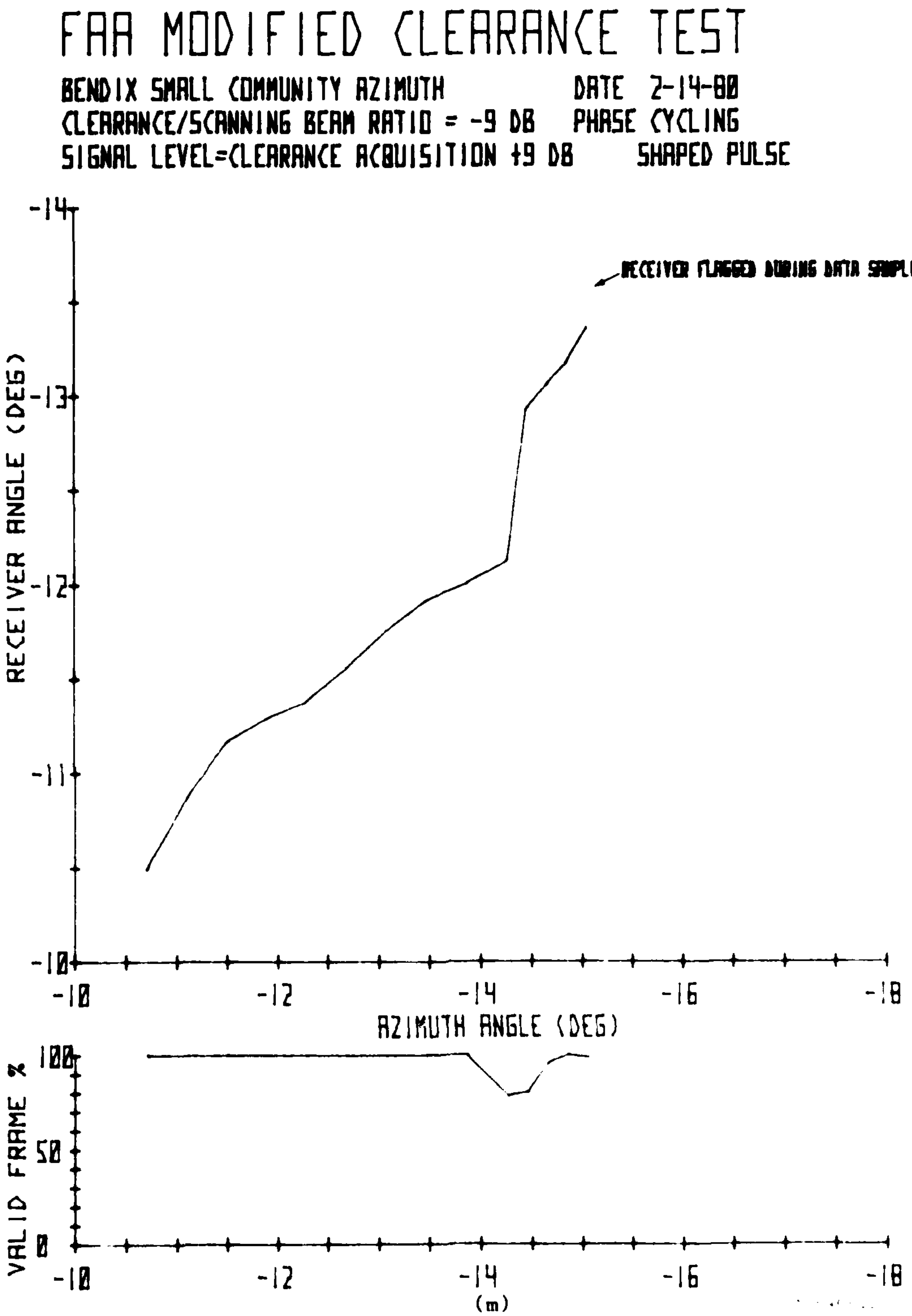

FIGURE 12. AZIMUTH RECEIVER ANGLE VERSUS TRUE AZIMUTH PLOTS USING THE SHAPED CLEARANCE PULSE (SHEET 13 OF 15)

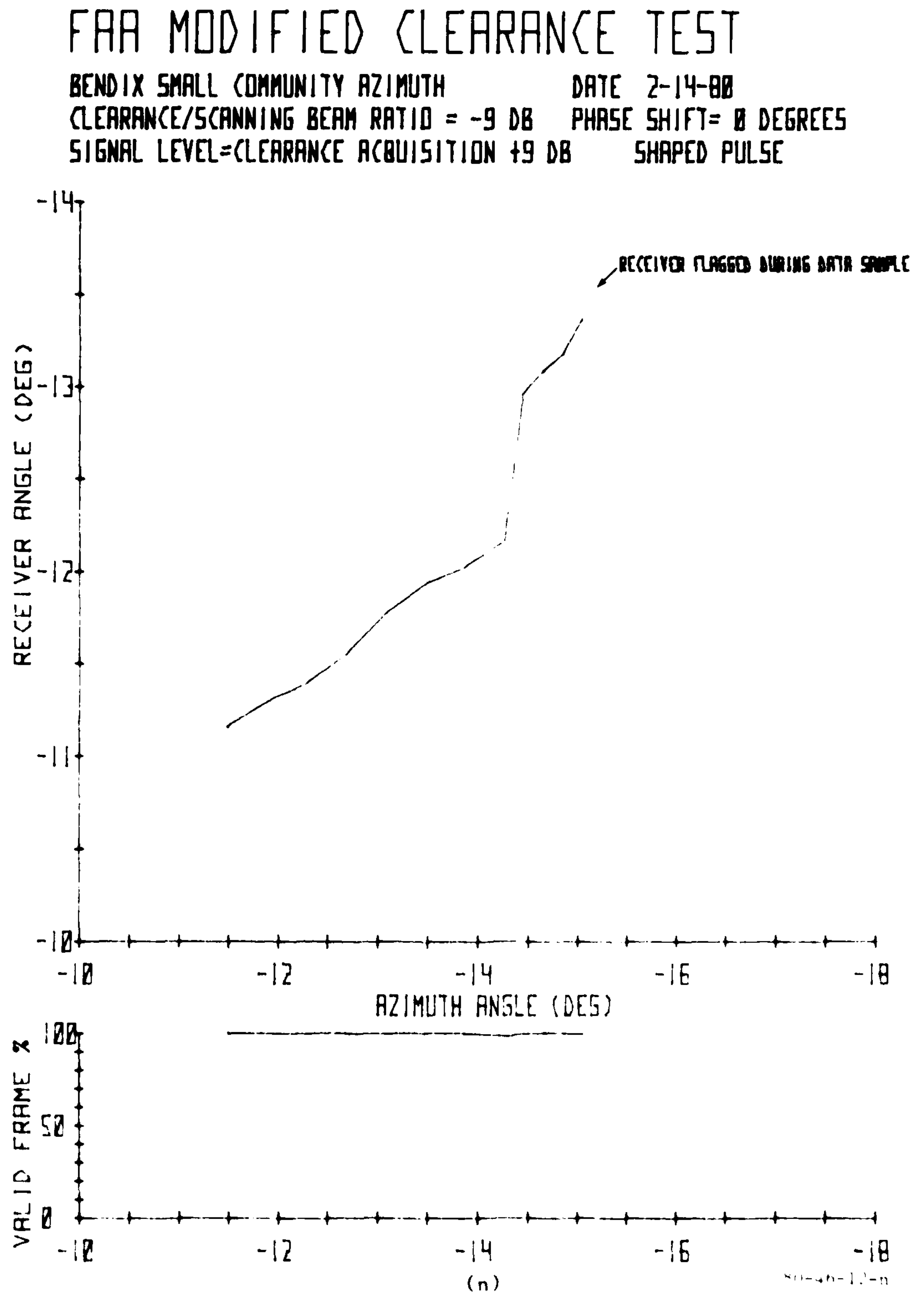

FIGURE 12. AZIMUTH RECEIVER ANGLE VERSUS TRUE AZIMUTH PLOTS USING THE SHAPED CLEARANCE PULSE (SHEET 14 OF 15)

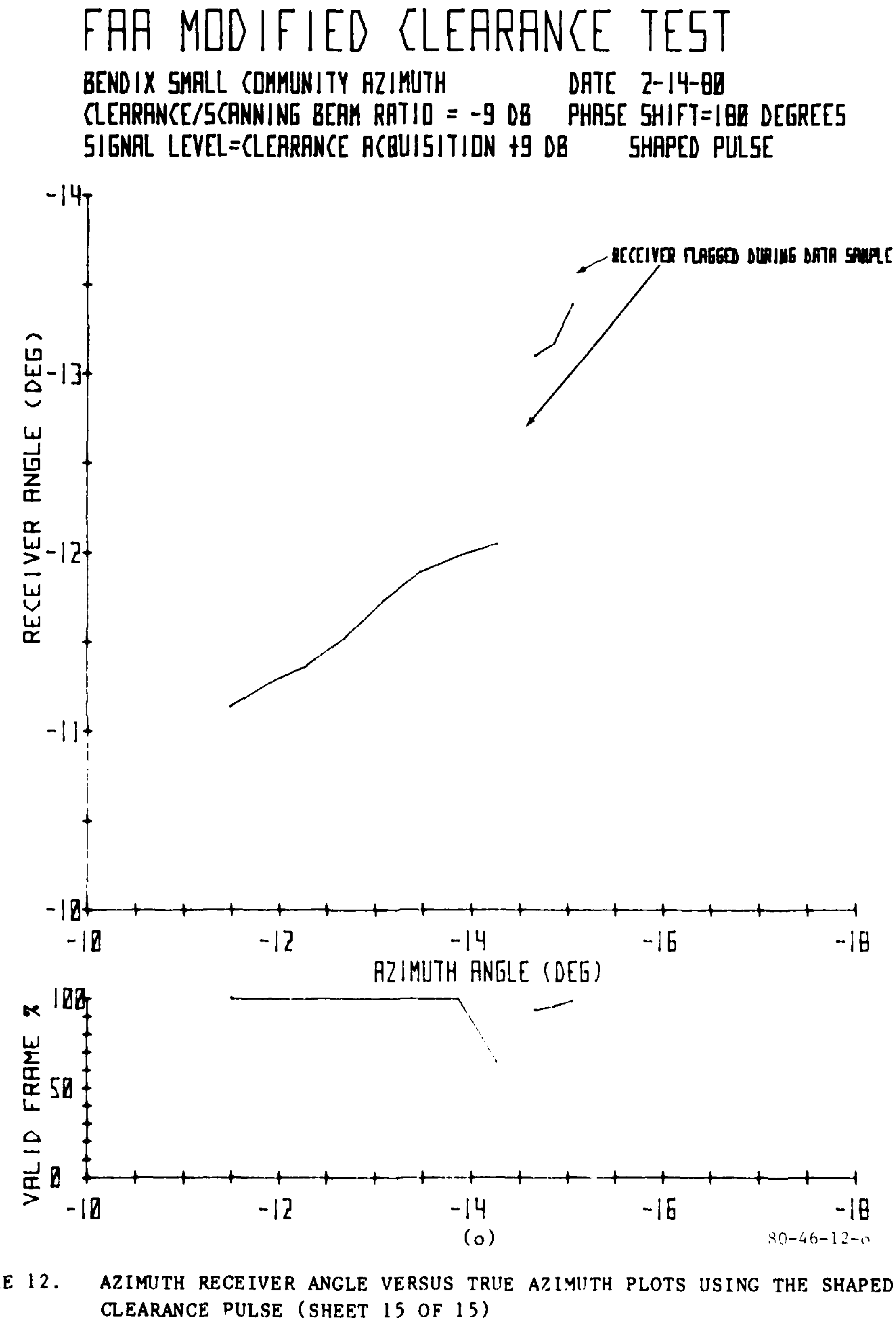

FIGURE 12. AZIMUTH RECEIVER ANGLE VERSUS TRUE AZIMUTH PLOTS USING THE SHAPED CLEARANCE PULSE (SHEET 15 OF 15)

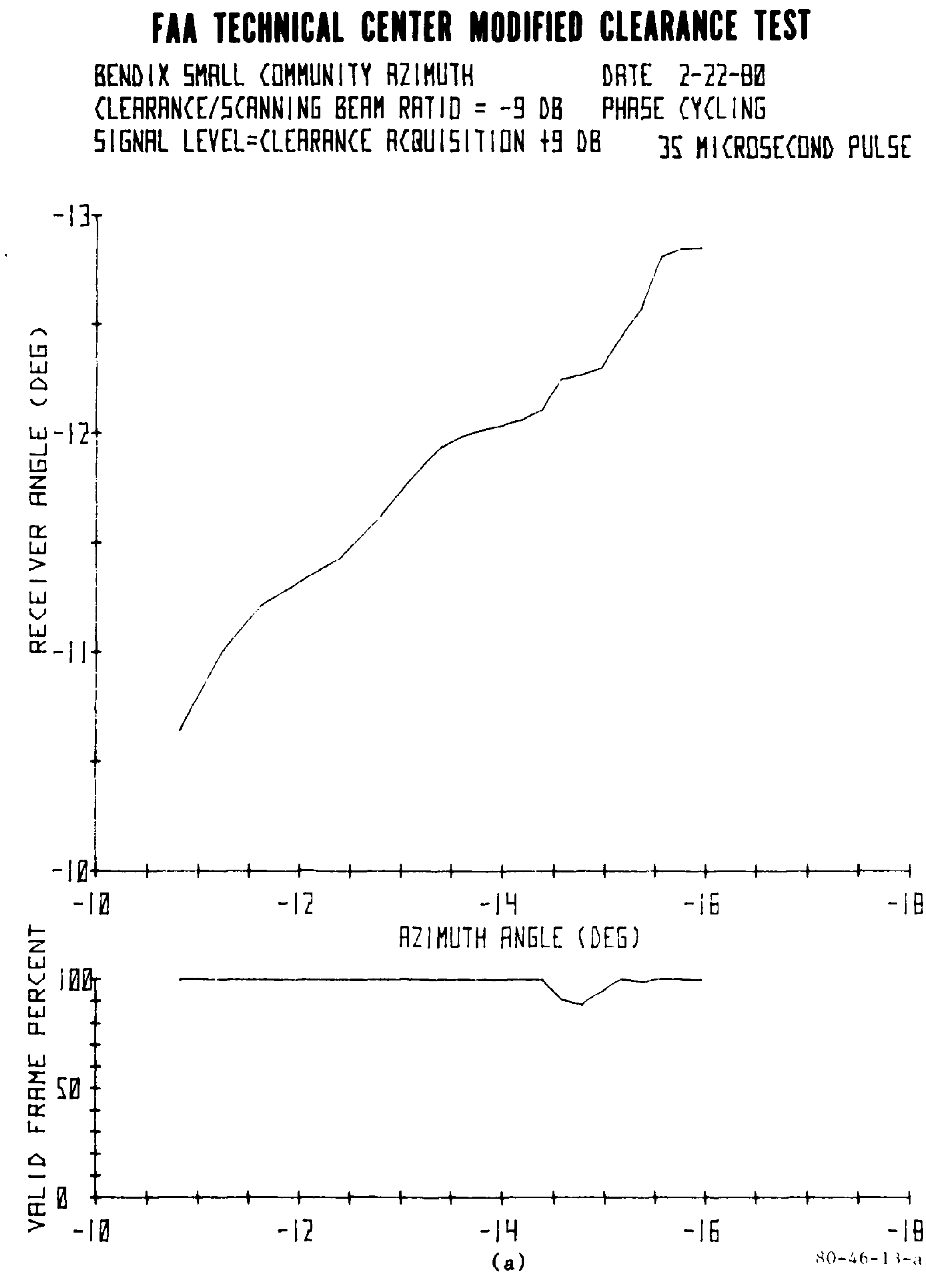

FIGURE 13. AZIMUTH RECEIVER ANGLE VERSUS TRUE AZIMUTH PLOTS USING THE 35 μs SQUARE PULSE (SHEET 1 OF 12)

FAA TECHNICAL CENTER MODIFIED CLEARANCE TEST

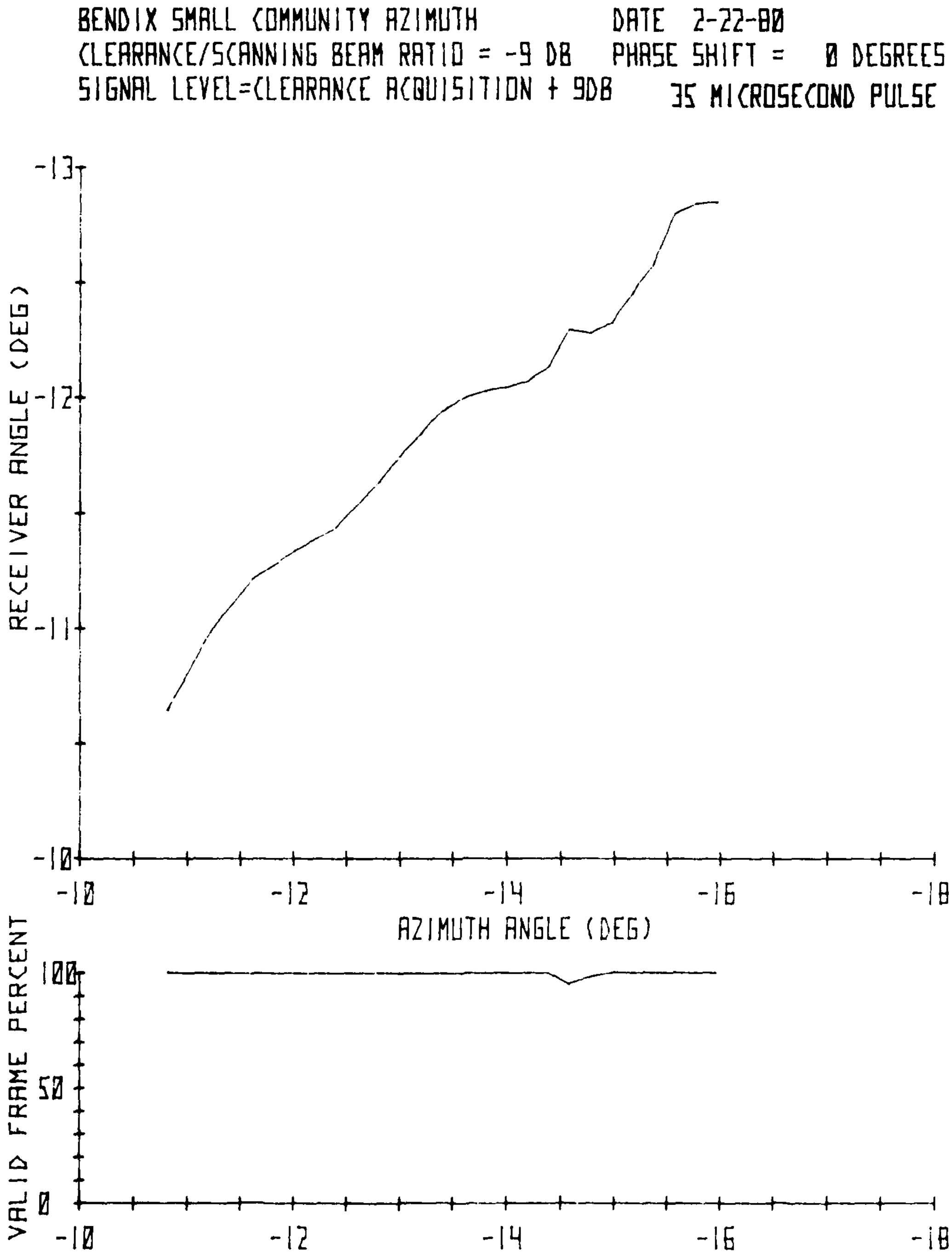

(b)

FIGURE 13. AZIMUTH RECEIVER ANGLE VERSUS TRUE AZIMUTH PLOTS USING THE 35 μs SQUARE PULSE (SHEET 2 OF 12)

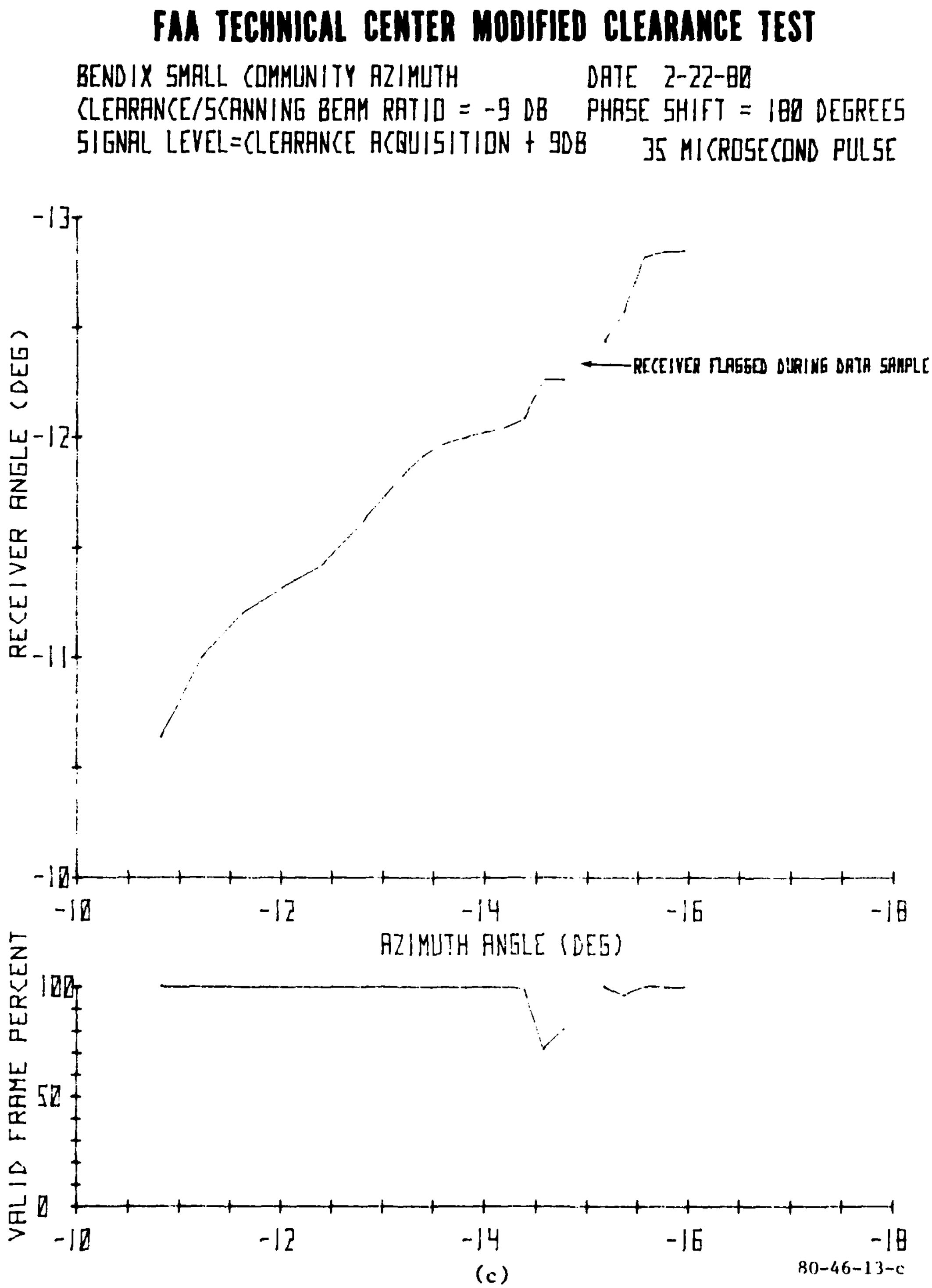

FIGURE 13. AZIMUTH RECEIVER ANGLE VERSUS TRUE AZIMUTH PLOTS USING THE 35 μs SQUARE PULSE (SHEET 3 OF 12)

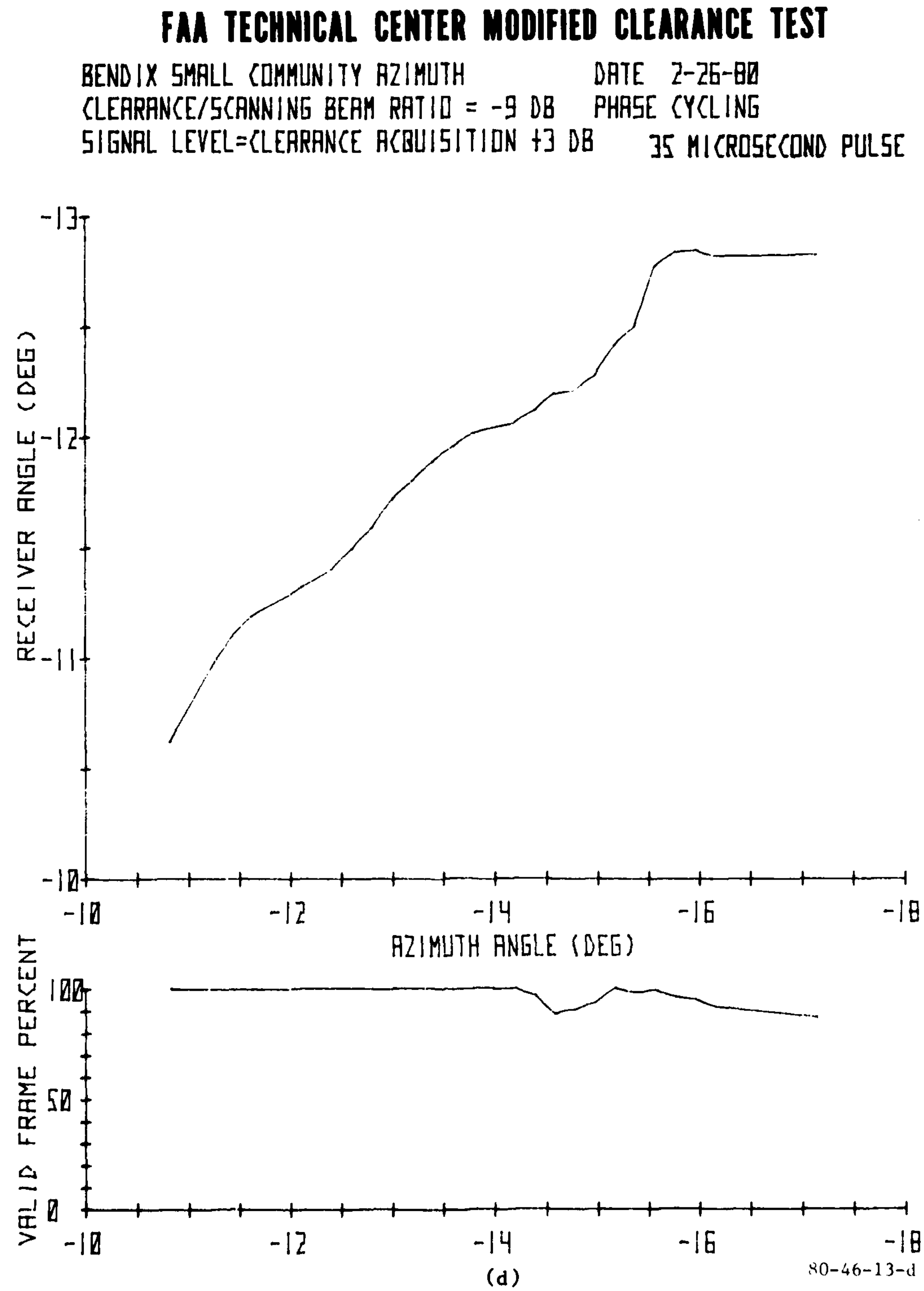

FIGURE 13. AZIMUTH RECEIVER ANGLE VERSUS TRUE AZIMUTH PLOTS USING THE 35 μs SQUARE PULSE (SHEET 4 OF 12)

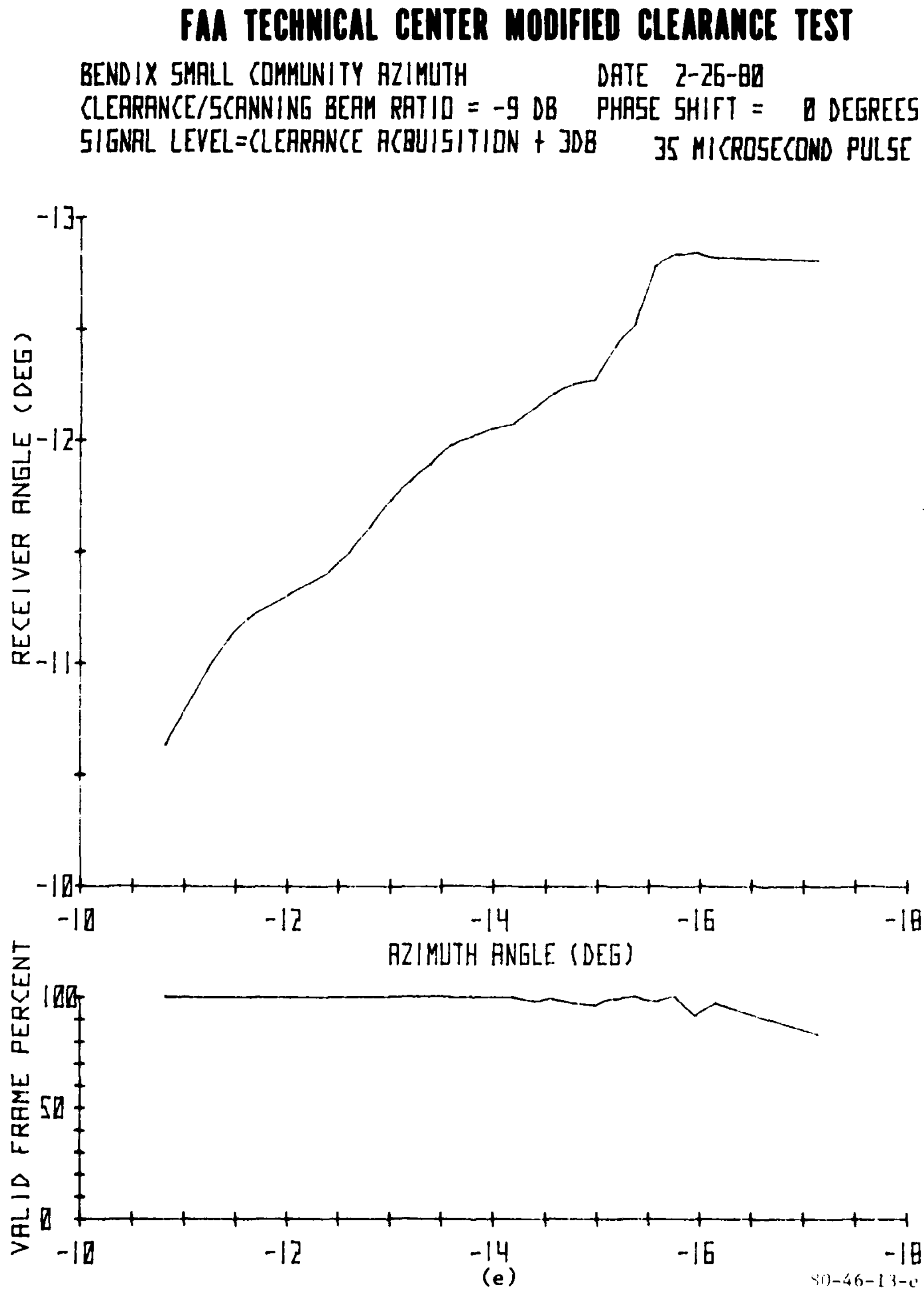

FIGURE 13. AZIMUTH RECEIVER ANGLE VERSUS TRUE AZIMUTH PLOTS USING THE 35 μs SQUARE PULSE (SHEET 5 OF 12)

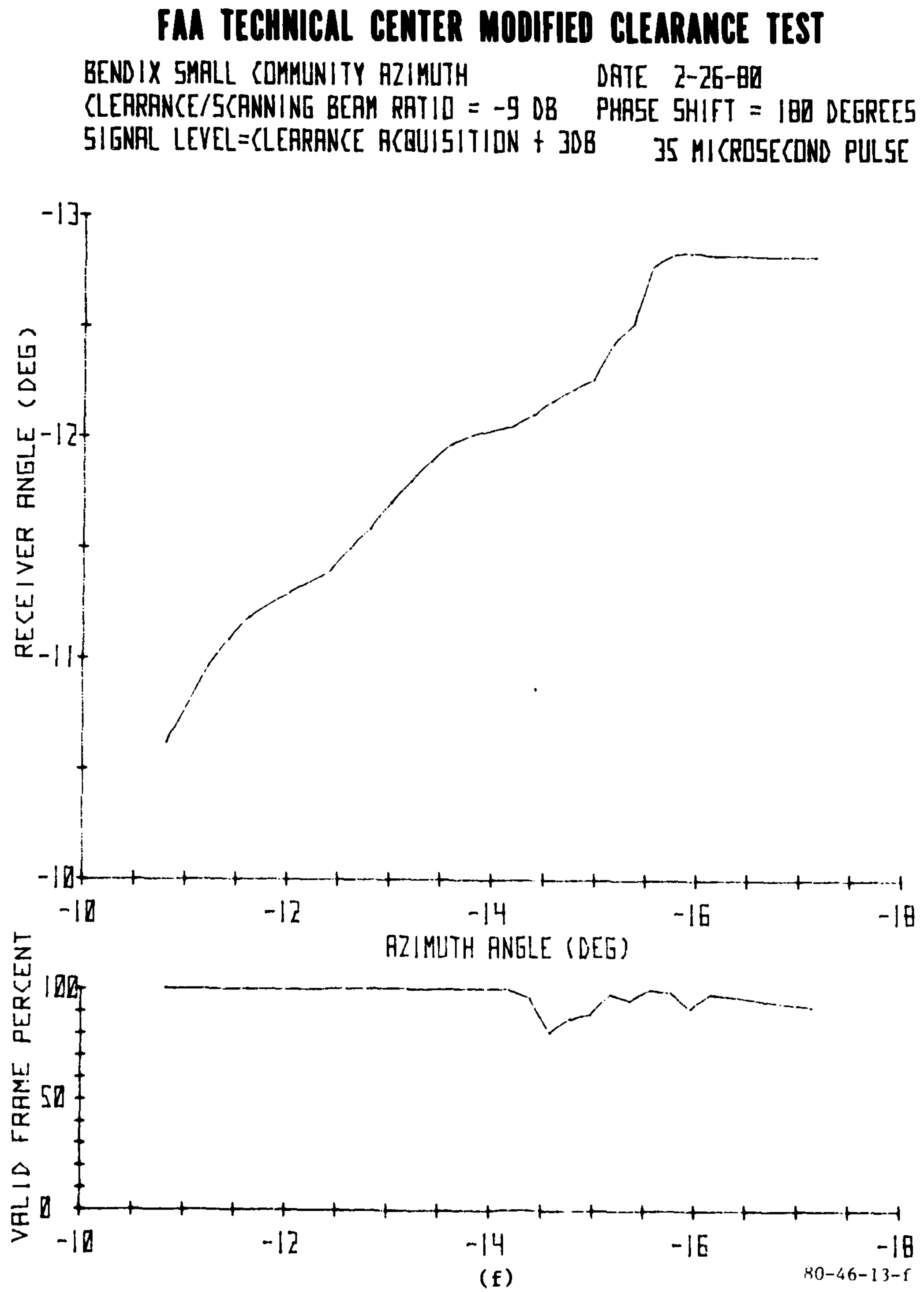

FIGURE 13. AZIMUTH RECEIVER ANGLE VERSUS TRUE AZIMUTH PLOTS USING THE 35 μs SQUARE PULSE (SHEET 6 OF 12)

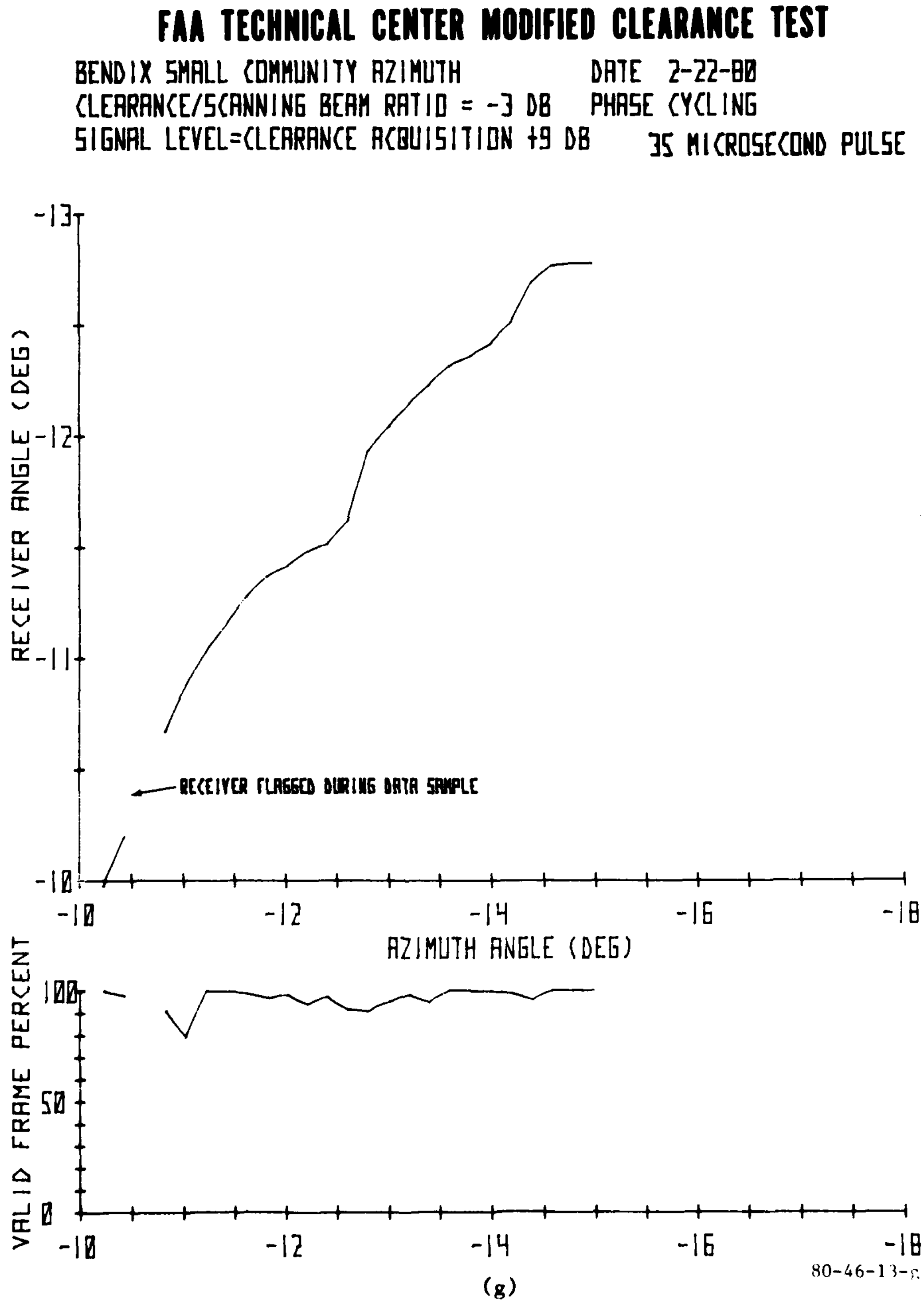

(g)

FIGURE 13. AZIMUTH RECEIVER ANGLE VERSUS TRUE AZIMUTH PLOTS USING THE 35 μs SQUARE PULSE (SHEET 7 OF 12)

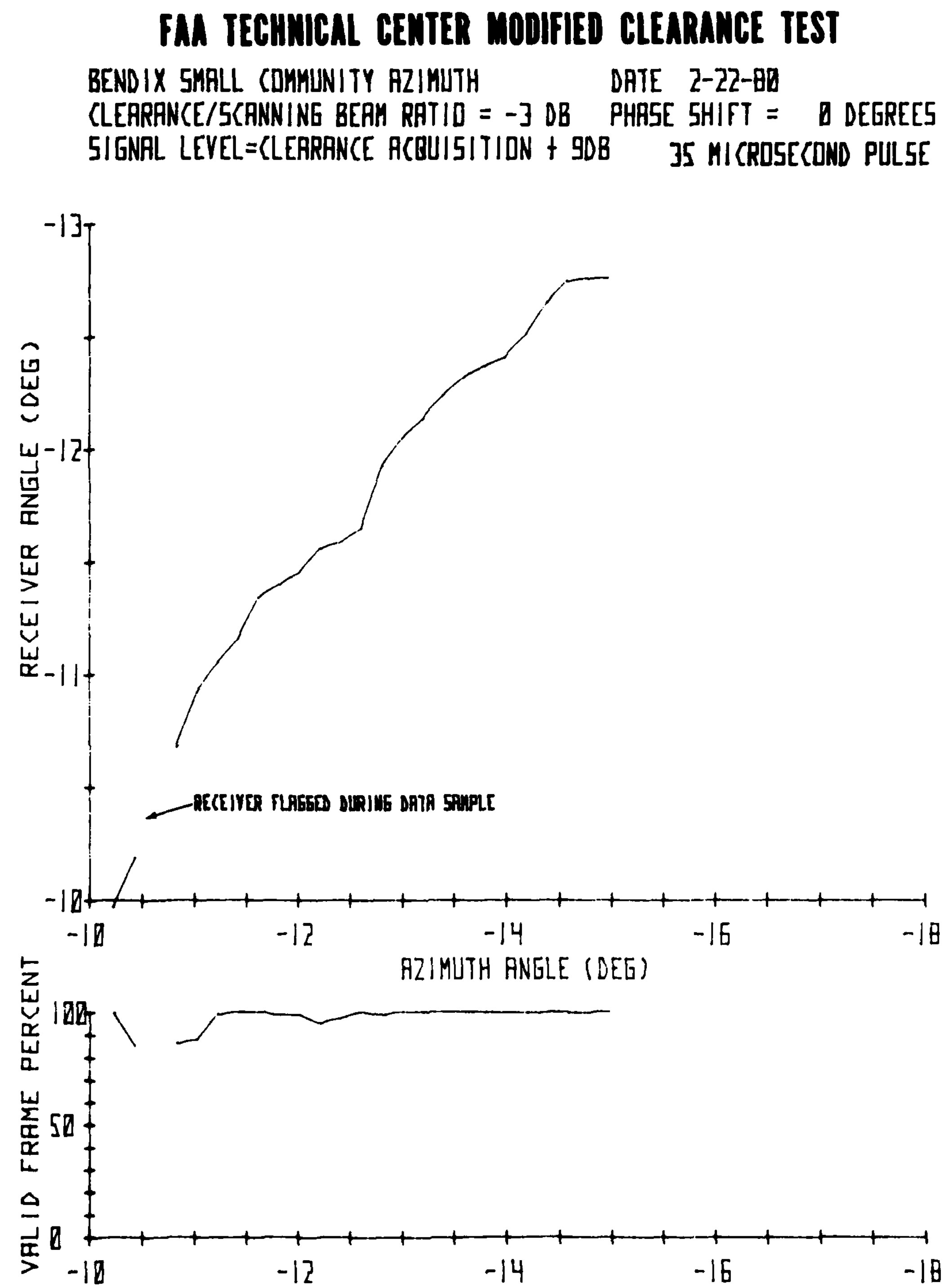

(h)

80-46-13-h

FIGURE 13. AZIMUTH RECEIVER ANGLE VERSUS TRUE AZIMUTH PLOTS USING THE 35 μs SQUARE PULSE (SHEET 8 OF 12)

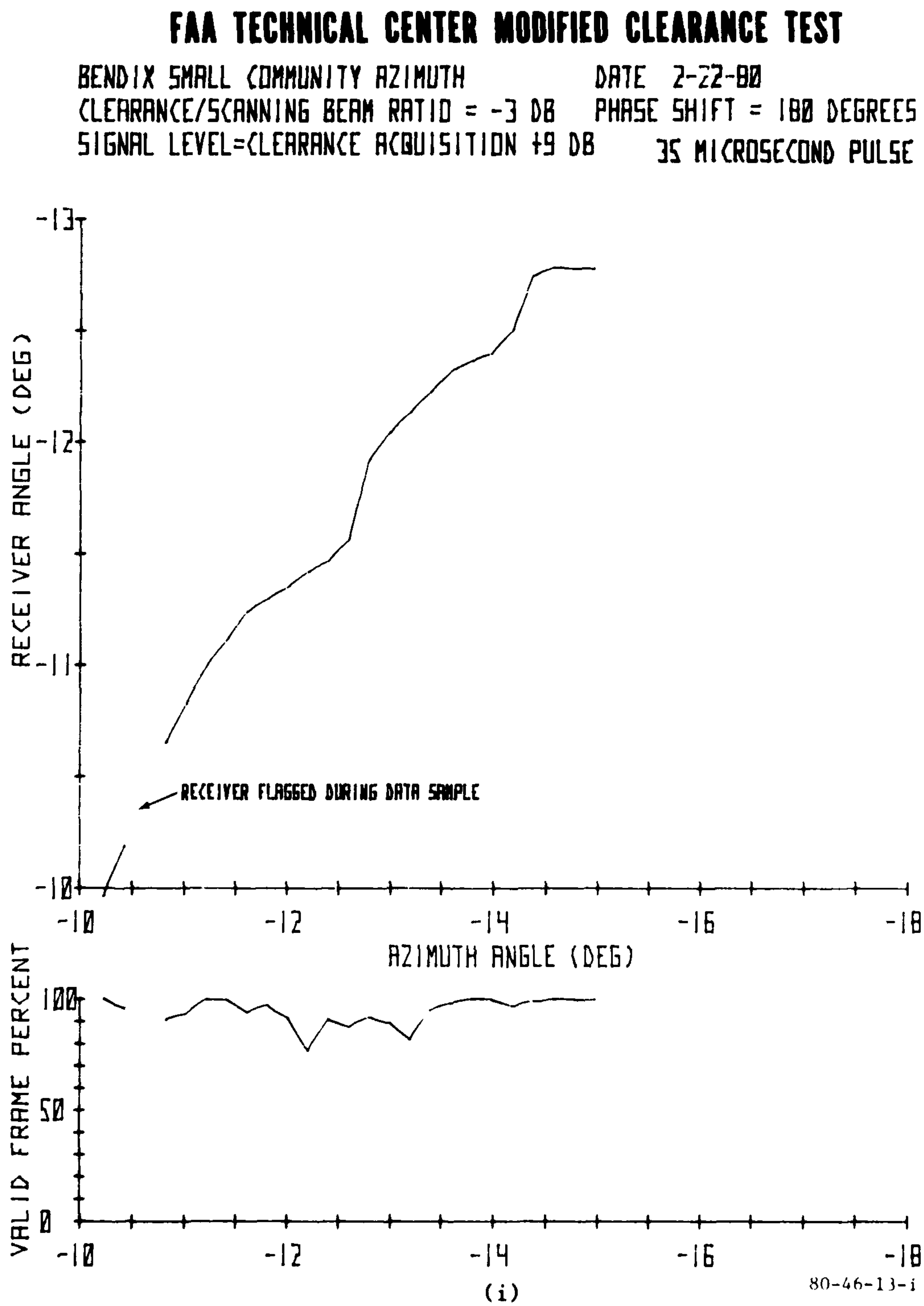

FIGURE 13. AZIMUTH RECEIVER ANGLE VERSUS TRUE AZIMUTH PLOTS USING THE 35 μs SQUARE PULSE (SHEET 9 OF 12)

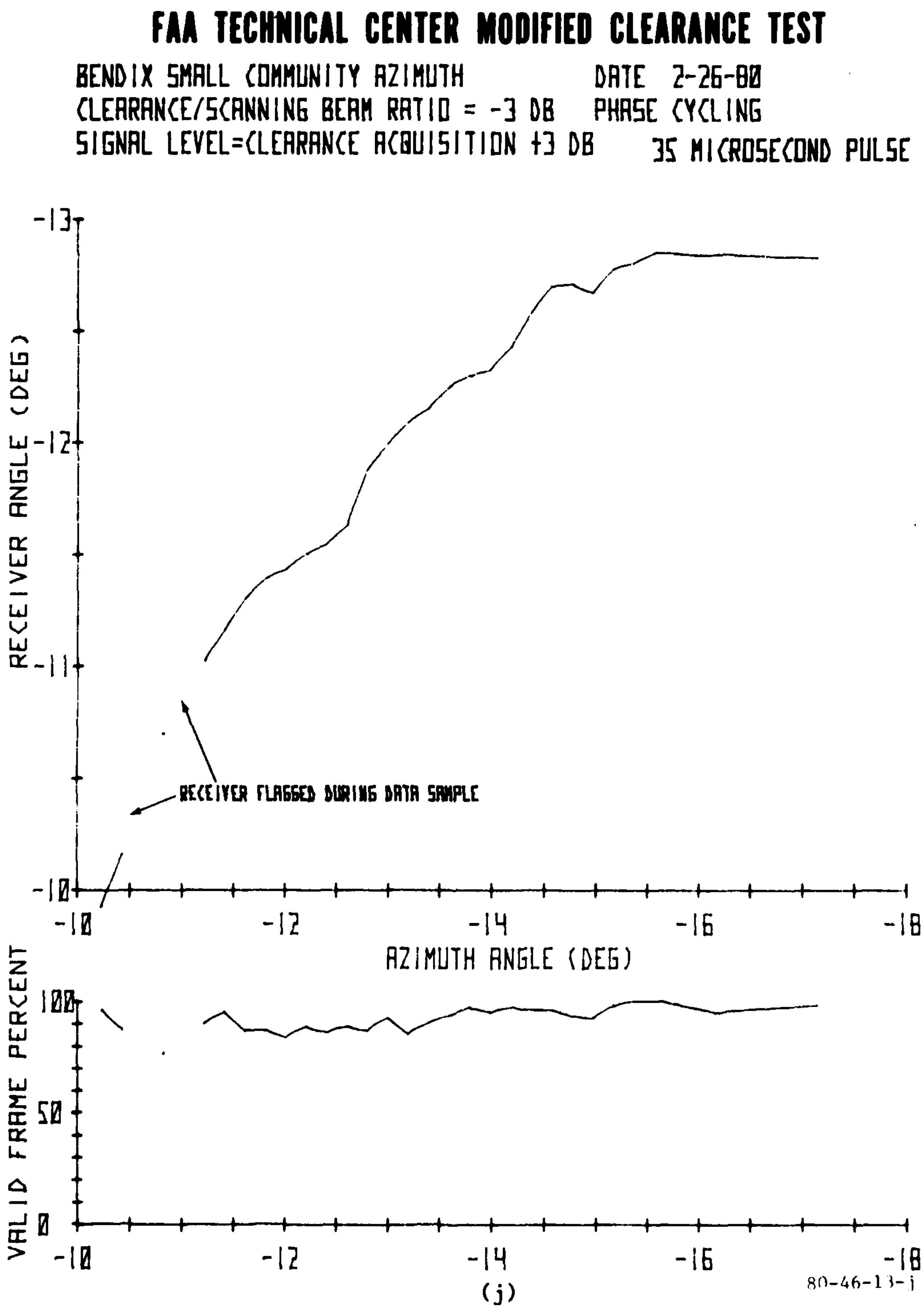

FIGURE 13. AZIMUTH RECEIVER ANGLE VERSUS TRUE AZIMUTH PLOTS USING THE 35 μs SQUARE PULSE (SHEET 10 OF 12)

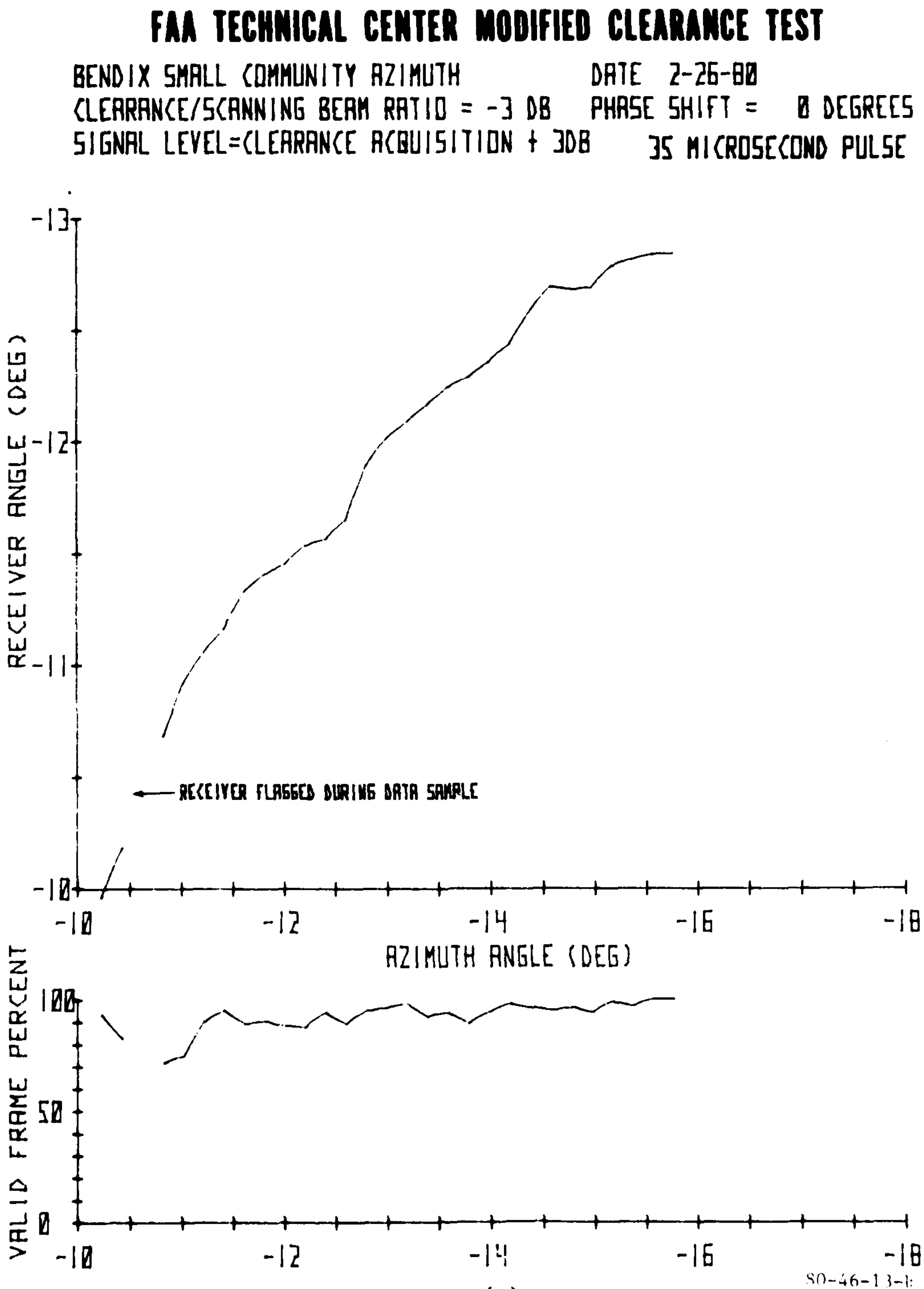

(k)

FIGURE 13. AZIMUTH RECEIVER ANGLE VERSUS TRUE AZIMUTH PLOTS USING THE 35 μs SQUARE PULSE (SHEET 11 OF 12)

FAA TECHNICAL CENTER MODIFIED CLEARANCE TEST

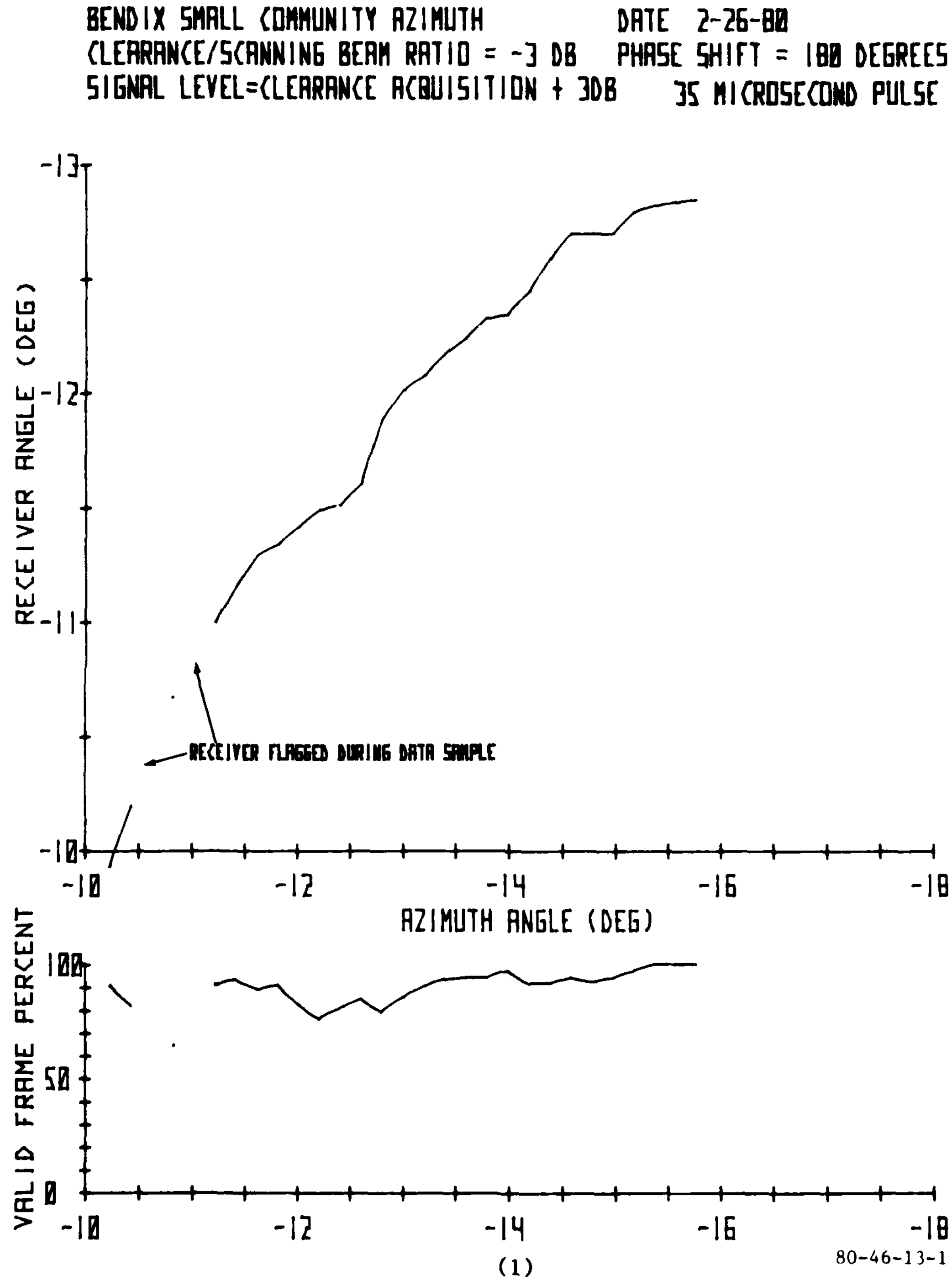

FIGURE 13. AZIMUTH RECEIVER ANGLE VERSUS TRUE AZIMUTH PLOTS USING THE 35 μs SQUARE PULSE (SHEET 12 OF 12)

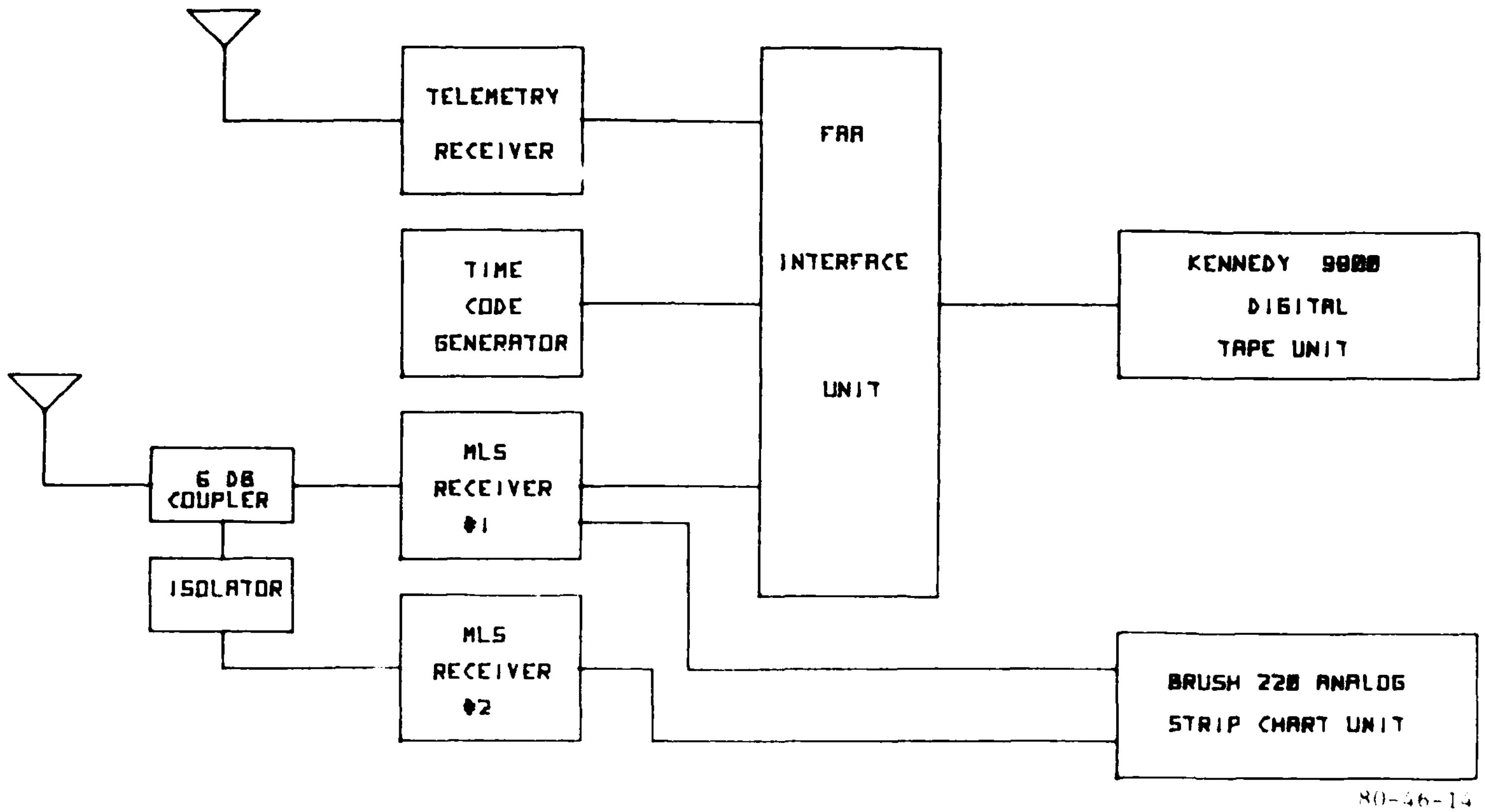

FIGURE 14. MLS TEST AIRCRAFT DATA COLLECTION PACKAGE BLOCK DIAGRAM

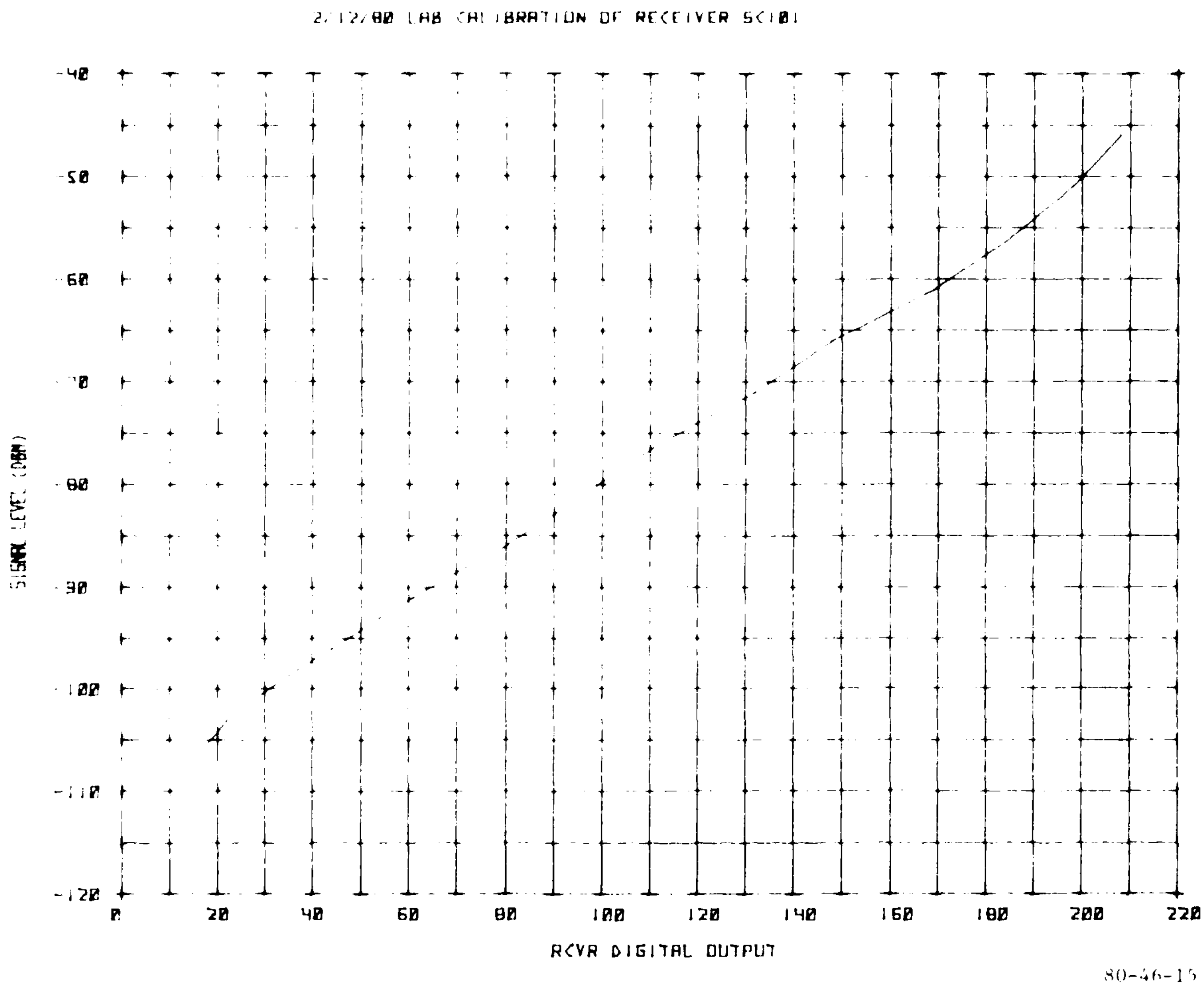

FIGURE 15. RECEIVER CALIBRATION CURVE (S/N SC101)

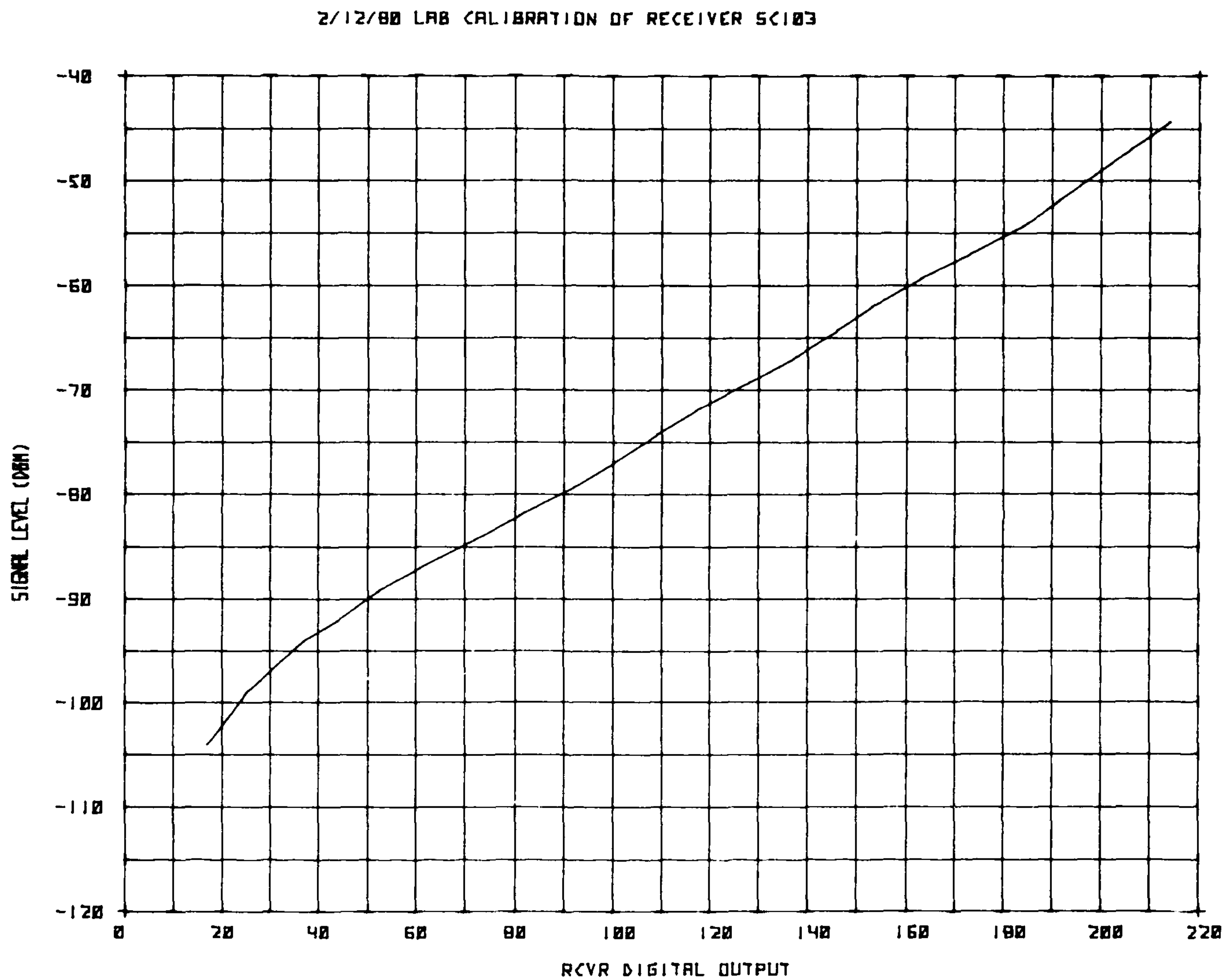

80-46-16

FIGURE 16. RECEIVER CALIBRATION CURVE (S/N SC103)

TABLE 2. FLIGHT TEST SUMMARY

Date	Run	Flight Pattern	Altitude (ft)	Range (nmi)	Ground Station Configuration
2/6/80	2 and 3	"S" shaped radial (-10° to -15°)	4,500	From 20	Site 1 (runway): proposed format, shaped pulse, phase incrementing in left clearance (CL), left and right CL amplitude unequal.
	4	CCW Partial Orbit (±50°)	3,500	10	
	5	CW Partial Orbit (±50°)	3,500	10	
2/8/80	1 and 2	"S" Shaped Radial (-10° to -15°)	4,500	From 20	Site 1: proposed format, shaped pulse, phase incrementing in left CL, left and right CL amplitude equal.
	4	CCW Partial Orbit (±50°)	2,000	6	
	5	CW Partial Orbit (±50°	2,000	6	
2/27/80	1	CW Partial Orbit (±50°)	2,000	6	Site 1: proposed format with 35 μs square pulse, phase incrementing in left CL, OCI's off, no attenuation.
	2	CCW Partial Orbit (±50°)	2,000	6	
	3 and 4	"S" Shaped Radial (-10° to -15°)	2,000	12	
	6*	CW Partial Orbit (±50°)	2,000	6	Same as runs 1 to 4 except no phase incrementing.
	7	CW Partial Orbit (±50°)	2,000	6	
	8	"S" Shaped Radial (-10° to -15°)	2,000	12	
2/28/80	1	CW Orbit (±50°)	1,500	6	Site 1: existing format, no modification.
	2	CCW Orbit (±50°)	1,500	6	
	4 and 5	"S" Shaped Radial (-10° to - 15°)	1,500	11	
3/4/80	1*	CW Orbit 0° to 35°	1,600	6	Site 2 (Hangar): existing format.
	2*	CCW Partial Orbit 30° to 0°	1,600	6	
	3*	CW Partial Orbit 0° to 35°	1,600	6	
	4*	"S" Shaped Radial (11° to 17°)	1,600	12	
3/5/80	1	"S" Shaped Radial (11° to 17°)	4,000	20	Site 2: existing format.
	2	"S" Shaped Radial (11° to 17°)	4,000	20	Site 2: proposed format with 35 μs pulse.
	3	"S" Shaped Radial (11° to 17°)	1,600	12	
	4	CW Orbit 0° to 35°	1,600	6	
	5	CCW Orbit 35° to 0°	1,600	6	
3/6/80	1	"S" Shaped Radial (11° to 17°)	4,500	20	Site 2: proposed format with 35 μs pulse, no phase incrementing, OCI's on.
	2 and 3	"S" Shaped Radial (14°± 1°)	1,600	12	
	4	CW Partial Orbit 0° to 35°	1,600	6	
	5	CCW Partial Orbit 35° to 0°	1,600	6	
	6	"S" Shaped Radial (-11° to -16°)	4,500	20	
	7	"S" Shaped Radial (-14° ± 1°)	1,600	12	
	9	"S" Shaped Radial (14° ± 1°)	1,600	12	Site 2: existing format.

*No Nike Tracking

ATE

LME